SHIELDING EFFECTIVENESS ESTIMATION

Guillaume Girard

A Thesis

In

The Department of Electrical Engineering

Presented in Partial Fulfillment of the Requirements for the Degree of
Master of Applied Science in Electrical Engineering
Concordia University
Montreal, Quebec, Canada

August 2002

ABSTRACT

SHIELDING EFFECTIVENESS ESTIMATION

Guillaume Girard

The application of SE estimation methods for small enclosures is the main subject of this thesis. Three Shielding Effectiveness estimation methods are presented; Empirical, Experimental and Numerical Simulation. SE estimates have been compared with SE measurements showing close correlations between the numerical simulation and the experimental results. It has been proved that the SE of an empty enclosure, compared with that of an enclosure containing a printed circuit board, differs due to volume change, herein Q variation. Conclusions are formulated in terms of further works to be accomplished in order to determine better measurement and simulation models for Shielding Effectiveness estimates.

ACKNOWLEDGEMENTS

Many thanks to Dr. C. W. Trueman for his supervision, professional support and the use of is FDTD code. I would also like to acknowledge the constant support of C-MAC Engineering (Jacques Rollin) and Dr. David Johns, from Flomerics Inc., for the Flo-EMC (TLM) software.

Thank you to my parents, Gaston and Suzanne Girard for their support. A big thanks, to Rose Pradieu for the soul food that energized me during research time and Fabiola Pradieu for moral support.

TABLE OF CONTENTS

TABLE OF FIGURES

TABLE OF TABLES

CHAPTER 1

INTRODUCTION

1.1 Electromagnetic Compatibility

Any electrical device that operates normally in an electrical environment without causing any interference is said to be "Electromagnetic Compatible". Meeting the Electromagnetic Compatibility (EMC) requirements for high-speed digital equipment, without a shielded enclosure, is a very difficult, almost impossible, task. The shielding provides isolation between the electromagnetic field inside an enclosure and outside the enclosure. Shielding is necessary to prevent the circuit in an enclosure to radiate fields that will interfere with the operation of other devices. The shielding also helps to prevent interference, from external fields, with the operation of the device under design.

There are regulations restricting the "Radiated Emissions" and demanding "Immunity". Shielding is accomplished, ideally, by enclosing the electrical device in a solid, perfectly conducting, metal box, with no holes, that behaves like a "Faraday Cage". A shield should also provide perfect isolation between the inside and outside of the box. Most metal boxes, available on the market, with holes for cables and other accessories, provide imperfect shielding.

Slots, apertures, ventilation holes, I/O cables and power lines, etc, always compromise the integrity of the shield. [1] Frequently, mechanical engineers do not estimate, or take into account, the amount of shielding lost via those imperfections.

Normally, only the intrinsic Shielding Effectiveness (SE) value of a material, is taken into account, in the design process. For the enclosure, it is the overall shielding that counts, neglecting the above mentioned imperfections in a shielded enclosure, can and will result in inadequate shielding, costly re-design, and can postpone the date for the introduction of the product on the market.

Considering that SE is the amount of attenuation a shield can offer, then, SE of an enclosure must be quantified in dB. Shielding Effectiveness is defined as the ratio of the field strength with the enclosure, divided by the field strength with no enclosure. The shielding is used to meet radiated emissions and radiated immunity EMC requirements.

Many textbooks apply Shielding Effectiveness to a metal wall, but the wall is not part of the definition. It is simply used to illustrate the use of the formula by which the amount of shielding is quantified. Shielding of a conductive surface is usually determined by the addition of its [7][18]:

reflection loss (R), absorption loss (A) and multiple reflection loss (M)

within the conductive sheet of material on which an incident electromagnetic field strikes;

$$SE = R + A + M. \quad \text{(dB)} \tag{1-1}$$

Results obtained from this equation do not represent the real values of SE for an enclosure. Generally, it is much higher (>40 dB). In other words, SE of a metal panel is much, much higher than the SE of an enclosure, made of six metal panels, because fields "leak in" through holes and openings. From design experiences and previous studies, [2][3][4], it was found that geometric slots, apertures, vents holes, resonance cavities, and any major openings in the shield, are the dominant factors to characterize shield attenuation. Many kinds of apertures, slots, seams and resonant cavities, have been examined in previous studies [2][3][4]. Those equations can be applied to the shielding of enclosures with a little bit of work. The information obtained, can be very useful at the beginning of the design process, in order to establish dimensions, to restrict opening lengths in order to eliminate any possible antenna or resonance effects.

EMC regulatory requirements are not rules to follow when designing an enclosure; it is a pass-fail criterion, since there are certain levels of emissions electronic devices must meet. These can only be determined by testing. The only way a designer can build a good EMC enclosure is by working with an EMC budget, in which the specific amount of shielding needed to meet the EMC requirement limits is set.

Such a budget is done at the beginning of a project, when most of the information is still unknown. Values are chosen arbitrarily at this stage. Further down, at different stages, during the development process, studies of the enclosure are done to evaluate the SE of the enclosure and to realign the design strategies.

By following an EMC budget and SE estimation, engineers will have more confidence in the final design. Changes to the enclosure design can be very costly at the end of the design process. Last-minute changes can delay the marketing of the product. In today's competitive markets, no one can take such a chance!

1.2 Objective

The objective of this thesis is to introduce simple SE estimation methods, used in the industry, for designing shielded enclosures. Each method will be explained in detail and applied to a simple enclosure model. The pros and cons of each analysis technique will be discussed. Cross-references to the EMC design process and / or EMC budget will also be examined for optimization of the design.

1.3 Contribution

The contribution of this thesis, is the application of SE estimation methods for small enclosures. SE estimates will be compared with SE measurements using an industry-standard test method, and with computations of the SE using two well-known methods. The thesis will compare the SE of an empty enclosure with that of an enclosure containing a printed circuit board (PCB). No previous studies have described and compared methods for Shielding Effectiveness estimation of small enclosures in a design process. This thesis introduces, as a second contribution, an industry accepted test method for Shielding Effectiveness, using the reciprocity theorem.

Other estimation techniques for SE exist. However, it is believed, that the ones presented in this thesis, are the most frequently used, proven and cost effective.

1.4 Thesis Structures and Limitations

Three Shielding Effectiveness estimation methods will be studied:

(a) empirical, (b) experimental and (c) numerical simulations .

Each method will be described in details. The three methods will be applied to a simple electronic Aluminum enclosure, for SE comparisons. Two test case studies:

(a) the aluminum enclosure, containing a printed circuit board ,

and

(b) the aluminum enclosure not containing a printed circuit board,

are investigated using each method. Analysis of results will be done for each individual SE estimate method. The SE estimation method will be referenced to the general EMC design process. Comparisons of each SE estimation method will be performed to determine information available from each, and correlations between them.

This thesis is structured to focus on SE estimation methods for design and qualitative values of small enclosures. Further detailed work on noise source properties and numerical modeling for SE estimate, should be investigated as a complement to this thesis.

CHAPTER 2

SHIELDING EFFECTIVENESS AND EMC DESIGN

Achieving Electromagnetic Compatibility (EMC) is one of the biggest challenges in designing electrical devices. The best way of ensuring compatibility is to follow a proper EMC design process, which will include an EMC budget.

2.1 EMC Design

The EMC design objectives are to identify noise sources and their field strengths, identifying areas of the system where electromagnetic disturbances can emit from and mitigating this electromagnetic disturbance, by good EMC design practices. [39]

The EMC budget is one of the key items in the EMC design process. It is used to determine the amount of shielding needed for an enclosure. [27]

In this approach, the goal is to control the radiated emissions, due to sources of Electromagnetic (EM) fields, on the device that is being built. The purpose of the shield is to prevent the EM emissions, from the printed circuit board, from getting out of the enclosure.

2.1.1 EMC Budget.

The EMC budget is a document that combines the relative contributions and apparent gain (loss) introduced by factors in the design: enclosure design, use of metallic I/O, PCB construction, etc. The approach starts with the applicable system-level EMC that limits requirements and apportion relative contribution to each factor from the system down typically to the circuit level. The overall device is limited to a certain level of emission, and that of the budget apportion part of the overall level to each sub-system. [39][27]

Based upon this, design limits are identified for several key factors (e.g. shielding effectiveness, ASIC, etc.) to provide guidance for the design engineers. An example of a short EMC design process, applicable to small enclosures, is presented in appendix A.

Once all critical parts of design are identified, one can establish targets (limits) for the Shielding Effectiveness via the budget. For example, the designer may want to design a simple controller unit, using a Ball Grid Array (BGA) chip (600MHz clock). First, the designer needs to know in which countries the device will be marketed. If the United States of America is selected, the device must comply with FCC Part 15, Subpart B. giving a limit 56.4 dB μ V/m ref. $1x10^{-6}$ V/m (see Figure 2-1, 2-2 and Table 2-1 for limit examples by country).

After consultation of BGA manufacturer's data sheets, one knows that the general emission level of the BGA at 600 MHz, is 80 dB μ V/m ref. $1x10^{-6}$ V/m. By

subtracting the limit value to this emission level one gets a shielding target of approximately 23.6 dB of Attenuation. In other words, permitted emission of 56.4 = BGA emission of 80 – shielding of 23.6. The thickness of the enclosure walls and the sizes of the holes can be decided using published formulas [1] to achieve a SE of 23.6 dB.

This thesis reviews shielding effectiveness measurement methods, that are used to evaluate the SE at various steps in the design process, in order to verify its conformance to the EMC budget limits.

2.1.2 EMC Standards

EMC Regulatory Limits are established by standards applicable to each country of interest. Meaning, if the product is to be marketed in a specific country, it is necessary to prove compliance to certain EMC standards applicable to this specific country, as in Table 2-1.

Table 2-1: EMC Standard by Country.

DISCIPLINE	COUNTRY OR REGION	REGULATORY SPECIFICATION	INDUSTRY SPECIFICATION
Emissions	USA	FCC Part 15 Subpart B	GR-1089-CORE
	Canada	ICES 003	None
	Europe	EN 300 386-2 (EN 55022)	None
Immunity	USA/Canada	None	GR-1089-CORE
	Europe	EN 300 386-2 (EN 55024)	None

Each standard has its own emission level limits. Figure 2-1 and 2-2 represent the FCC limits over the frequency range of 30 MHz to 10 GHz. For example, for a Class A system, the maximum field strength that is permitted to radiate, must be less than 49.5 dB μ V/m. ref. 1 μ V/m. from 30 MHz to 88 MHz, less than 53.5 dB μ V/m. ref. 1 μ V/m. from 88 MHz to 216 MHz, less than 56.4 dB μ V/m. ref. 1 μ V/m. from 216 MHz to 960 MHz and less than 60 dB μ V/m. ref. 1 μ V/m. from 960 MHz to 1 GHz.

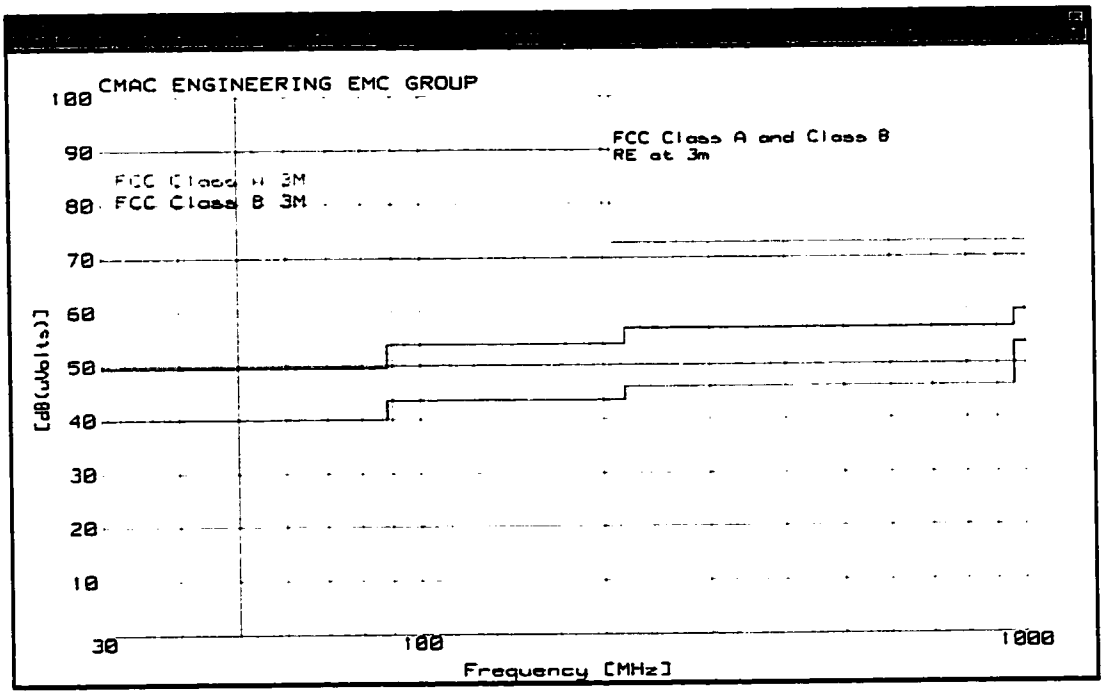

Figure 2-1: Radiated emission limits for FCC, 30 MHz to 1 GHz. [6]

The y-axis title should be read in dB μ V/m instead of dB μ V. This is a spelling mistake in the software. Class A is generally the limit for commercial devices and Class B for domestic.

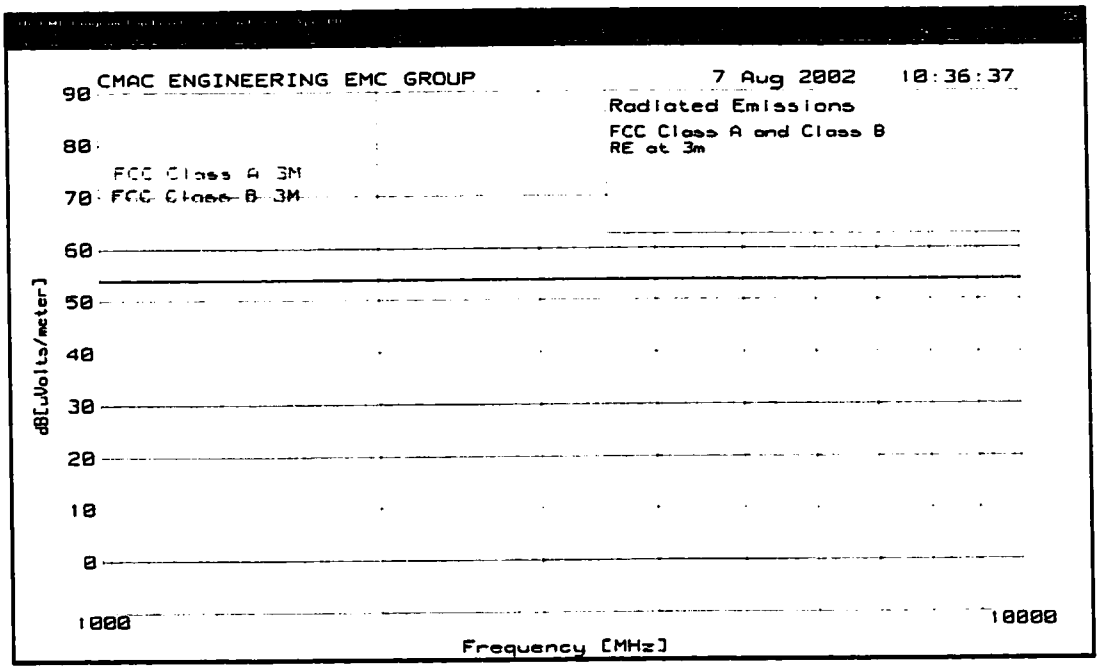

Figure 2-2: Radiated emission limits for FCC, 1 GHz to 10 GHz. [6]

2.2 Electromagnetic Interference

Electromagnetic interference problems consist of three basic components:

a source, a victim and a propagation path.

The sources of electromagnetic disturbances are numerous and can be both natural and / or man-made.

Atmospheric noises generated by electrical storms (below 10MHz) and solar radiations and cosmic noises (above 10MHz) are examples of natural sources. Man-made sources can be either intended or unintended. Intended sources are those that must radiate to perform their tasks (television, radio and radar). Licensing each radio station, TV station, and so forth, controls the field strengths emitted by "intended" sources. The license specifies the maximum fields that may be emitted and in which direction.

Unintended sources are electrical devices, like computers, switches, relays, appliances, power lines and many others. The purpose of radiated emissions standards is to limit the field strengths radiated by unintended sources.

The propagation paths of EMI can be either conducted or radiated. Conducted paths generally involve power lines or signal lines, connecting the source and the victim. Radiated interferences are more likely to appear on antenna to wire, wire to antenna coupling or wire to wire. Radiated EMI can also be coupled to cables going into a device, and conducted EMI can also radiate from cables going out of an electrical device. Finally, the victim can be any electrical man-made device. Figure 2-3 represents examples of EMI sources, paths and victims. [7][18]

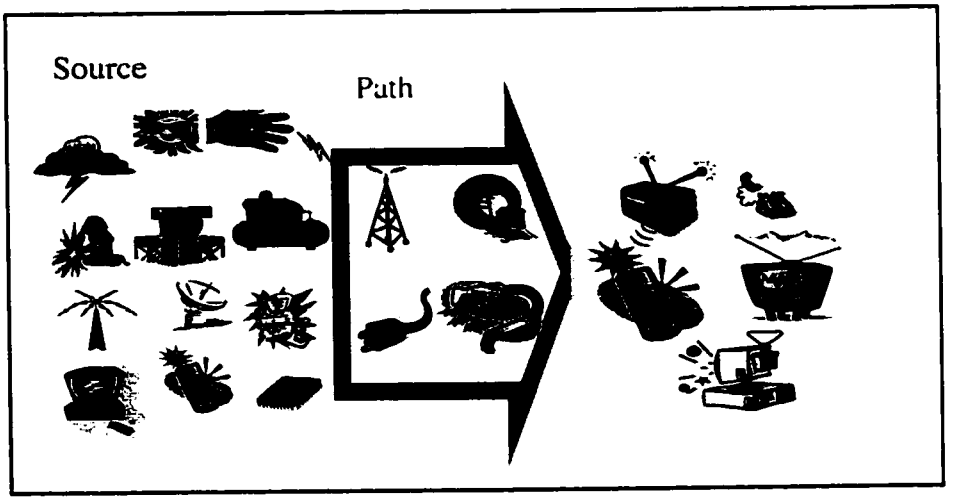

Figure 2-3: EMI component examples; source, path, victim. [7][39]

Electrical devices can present two types of EMI problems:

susceptibility or emission.

Figure 2-4 presents radiated emissions and susceptibility problems. In this study we will investigate more the 'emissions' side of the problem, but a designer must always remember that the immunity (susceptibility) is still a threat for his product.

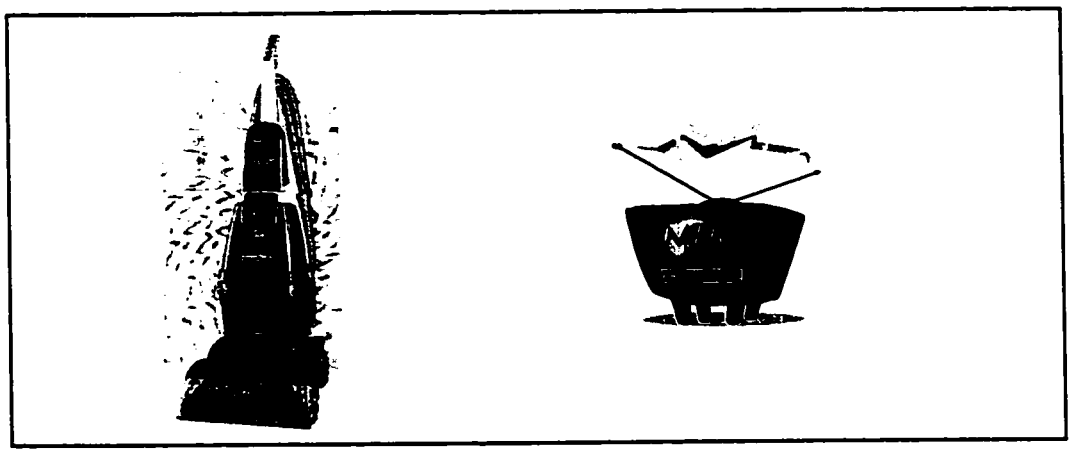

Figure 2-4: A) Radiated emission: the vacuum cleaner is an unintended radiator of electromagnetic noise B) Radiated immunity: the television set is susceptible to the vacuum cleaner electromagnetic noise creating white noise (snow) on its screen.

2.3 Shielding Effectiveness

Shielding Effectiveness, in general, for enclosures is defined as:

the amount of attenuation an enclosure provides.

The SE of an enclosure is, therefore, a measure of the Attenuation that a box or "shield" introduces. It is specified in terms of the reduction in electrical field strength and /or the field strength caused by the shield. For both, electric shielding effectiveness is defined as in Equation (2-1), (2-2), where E_0 is the incident field strength without the enclosure, and E_t is the field strength of the transmitted wave as it emerges from the

shield. Figure 2-5 is a physical representation of what is involved in equation (2- 1), (2-2) and presents the experimental formula for Shielding Effectiveness of small enclosure. In Equation (2-2): A is the field strength without the shield and B is the attenuated field strength with the shield in place. [5][7]

$$S = 20 \log (E_o / E_t) \text{ dB} \qquad (2\text{-}1)$$

$$SE = 20 \log (A) - 20 \log (B) \qquad (2\text{-}2)$$

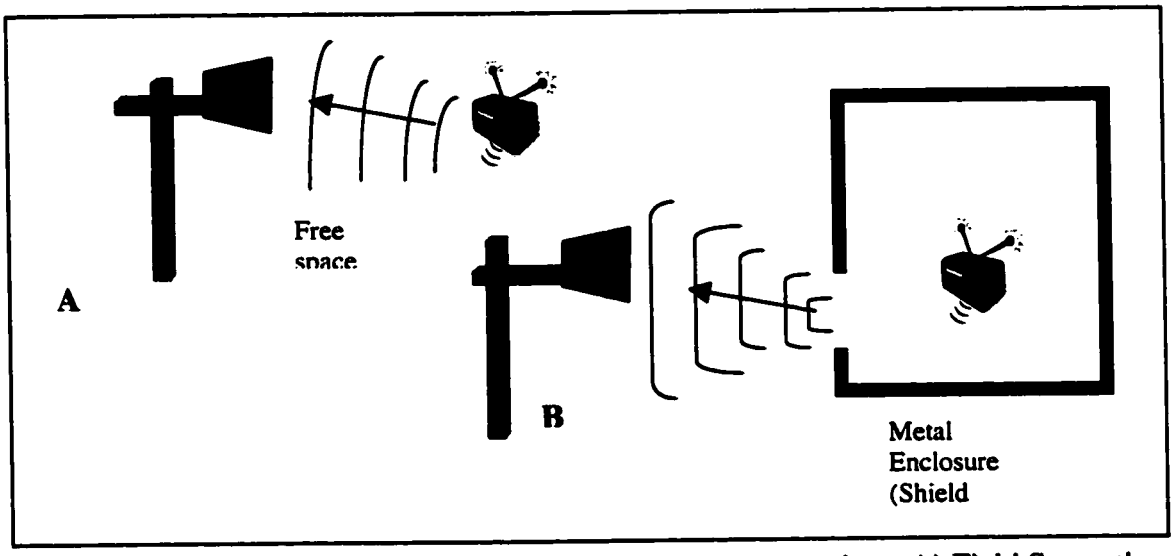

Figure 2-5: Shielding Effectiveness definition representation. A) Field Strength measurement coming out of a radio in free space B) Field Strength measurement of emission coming out of the box enclosing the radio.

Reciprocity should be pointed out at this stage concerning the SE definition. From previous studies, SE is used to refer to the case of an incoming plane wave and as a measurement or calculation of the field inside and outside the enclosure, as mentioned above in Equation (2-1) and (2-2). By reciprocity, radiated emission by which a noise

source alone (no shield/enclosure) radiates a field of E_{source}, the noise source inside the enclosure radiates (leaks) a field E_{box}, and the attenuation due to the enclosure is

$$A = E_{box} / E_{source}.$$

Since the experiment follows the reciprocity theorem, the "Shielding Effectiveness" and the 'attenuation' should be the same.

2.4 Empirical Formula for Shielding Effectiveness.

One of the first methods used to estimate SE was by empirical formulas. This method has been widely used in the past by design engineers and has been proven in the field [7]. However, assumptions and simplifications need to be made when using empirical methods, because of their limited accuracy.

One can also verify shielding effectiveness by measurements. Manufacturers use this method routinely. Standards have been written, with regard to testing material Shielding Effectiveness (e.g. MILSTD 285, SAE 1980 and IEEE-290). Military standards (MILSTD) were developed by the military for testing shielded enclosure integrity [8]. SAE 1980 and, IEEE290 are modifications of MILSTD285 with an approach over gaskets and material testing using the same principles. The standards and the Shielding Effectiveness definition are based on the exact mathematical analysis of an electromagnetic disturbance (plane wave) striking a conducting surface. [7][18][1]

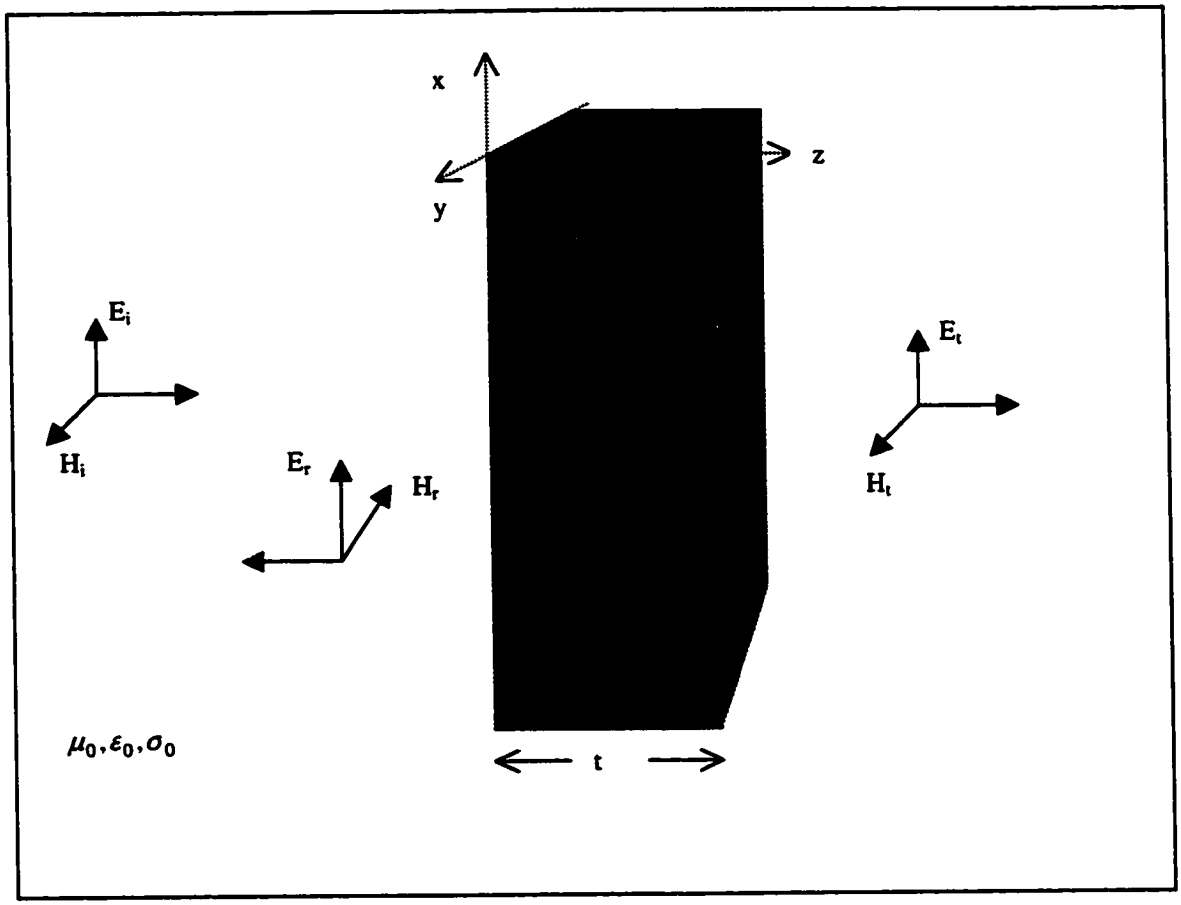

Figure 2-6: Plane wave striking a slab of conductive material. [18]

2.4.1 Shielding by a Thin Conductive Sheet.

Let's assume that a plane wave strikes a slab of conductive material, as in Figure 2-6. At the interface of the conductive surface three phenomena can occur:

1. Part of the incident plane wave is reflected from the conductive surface, giving rise to a reflected wave (E_r, H_r).
2. The incident wave is also partially absorbed by the material..
3. Internal reflection occurs inside the conductive material, due to the outer surface of the conductive slab.

The incident plane wave presented in Figure 2-6, can be defined by the following set of equations [7][18]:

$$\vec{E}_i = \hat{E}_i e^{-j\beta_0 z}\vec{a}_x \tag{2-3}$$

$$\vec{H}_i = \frac{\hat{E}_i}{\eta_0}\ e^{-j\beta_0 z}\hat{a}_y \tag{2-4}$$

where $\hat{E}$ is the complex amplitude of the vector field. The resulting initial reflecting field, after striking the conductive slab, should be reduced by a reflection coefficient (Γ) [7][17][18]:

$$\vec{E}_r = |\Gamma|\hat{E}_i e^{j\beta_0 z}\vec{a}_x = \hat{E}_r e^{j\beta_0 z}\vec{a}_x \tag{2-5}$$

$$\vec{H}_r = |\Gamma|\frac{\hat{E}_i}{\eta_0}e^{j\beta_0 z}\vec{a}_y = \frac{\hat{E}_r}{\eta_0}e^{j\beta_0 z}\vec{a}_y \tag{2-6}$$

$$\Gamma = \frac{\eta - \eta_0}{\eta + \eta_0} \tag{2-7}$$

the intrinsic impedance and phase constant in free space are respectively [7][18]:

$$\eta = \sqrt{\left(\frac{j\omega\mu}{\sigma + j\omega\varepsilon}\right)} \tag{2-8}$$

$$\beta_0 = \omega\sqrt{\varepsilon_0\mu_0} \tag{2-9}$$

For a good conducting material the intrinsic impedance can be expressed by

$$\eta = \frac{1+j}{\sigma\delta} \tag{2-8}$$

where δ , is the skin depth of the conductive slab [18]:

$$\delta = \sqrt{\frac{2}{\omega\mu\sigma}} \tag{2-9}$$

The waves at the first and second boundaries of the conductive slab can be described as [18]:

$$\vec{E}_1 = \hat{E}_1 e^{-j\kappa}\vec{a}_x \tag{2-10}$$

$$\vec{H}_1 = \frac{\hat{E}_1}{\eta_0} e^{-j\kappa}\vec{a}_y \tag{2-11}$$

$$\vec{E}_2 = \hat{E}_2 e^{-j\kappa}\vec{a}_x \tag{2-12}$$

$$\vec{H}_2 = \frac{\hat{E}_2}{\eta_0} e^{-j\kappa}\vec{a}_y \tag{2-13}$$

$$\gamma = \alpha + j\beta = \sqrt{j\omega\mu(\sigma + j\omega\varepsilon)} \tag{2-14}$$

The waves at the first and second boundaries of the conductive slab can be described as in Equation (2-17) and (2-18), where *t*, is the thickness of the conductive slab and δ , is the skin depth of the conductive slab, at a specific frequency. Inside the

material, the transmitted wave is attenuated due to the skin depth effect. The skin depth must always be less than the thickness of the material. The transmitted field is for $z \geq t$ [17][18]:

$$\vec{E}_{t2} = (1+\Gamma)\hat{E}_{t1} e^{-j\beta_0(z-t)} \vec{a}_x \tag{2-15}$$

$$\vec{E}_{t2} = (1+\Gamma)(1-\Gamma) e^{-\delta t} \hat{E}_{t1} e^{-j\beta_0(z-t)} \vec{a}_x \tag{2-16}$$

Enforcing the boundary conditions at z = *0* and z = *t*, we can determine the tangential components of the electrical and magnetic fields as:

$$\vec{E}_i\big|_{z=0} + \vec{E}_r\big|_{z=0} = \vec{E}_1\big|_{z=0} + \vec{E}_2\big|_{z=0} \tag{2-17}$$

$$\vec{E}_1\big|_{z=t} + \vec{E}_2\big|_{z=t} + = \vec{E}_t\big|_{z=t} \tag{2-18}$$

$$\vec{H}_i\big|_{z=0} + \vec{H}_r\big|_{z=0} = \vec{H}_1\big|_{z=0} + \vec{H}_2\big|_{z=0} \tag{2-19}$$

$$\vec{H}_1\big|_{z=t} + \vec{H}_2\big|_{z=t} + = \vec{H}_t\big|_{z=t} \tag{2-20}$$

By substitution, the following 4 equations are obtained:

$$\hat{E}_i + \hat{E}_r = \hat{E}_1 + \hat{E}_2 \tag{2-21}$$

$$\hat{E}_1 e^{-\gamma t} + \hat{E}_2 e^{-\gamma t} = \hat{E}_t e^{-j\beta_0 t} \tag{3-22}$$

$$\frac{\hat{E}_i}{\eta_0} - \frac{\hat{E}_r}{\eta_0} = \frac{\hat{E}_1}{\eta} - \frac{\hat{E}_2}{\eta} \tag{2-23}$$

$$\frac{\hat{E}_1}{\eta}e^{-\gamma t} - \frac{\hat{E}_2}{\eta}e^{-\gamma t} = \frac{\hat{E}_t}{\eta_0}e^{-j\beta_0 t} \tag{2-24}$$

Solving the four equations together gives the ratio of the incident and transmitted waves such as:

$$\frac{\hat{E}_i}{\hat{E}_T} = \frac{(\eta+\eta_0)^2}{4\eta\eta_0}\left[1-\left(\frac{\eta_0+\eta}{\eta+\eta_0}\right)^2 e^{-j2t/\delta}e^{-j2\beta t}\right]e^{jt/\delta}e^{j\beta t}e^{-j\beta_0 t} \tag{2-25}$$

Assuming a good conductor:

$$\frac{\eta_0-\eta}{\eta_0+\eta} \cong 1 \tag{2-26}$$

$$e^{-\gamma t} = e^{-\alpha t}e^{-j\beta t} = e^{-\frac{t}{\delta}}e^{-j\beta t} \le 1 \quad for \quad t \ge \delta \tag{2-27}$$

Substituting the above into equation (2-27) results in [18]:

$$\left|\frac{\hat{E}_i}{\hat{E}_t}\right| = \left|\frac{(\eta_0+\eta)^2}{4\eta\eta_0}\right|e^{t/\delta} \cong \left|\frac{\eta_0}{4\eta}\right|e^{t/\delta} \tag{2-28}$$

By taking the logarithm on both sides [7][18]:

$$SE_{dB} = 20\log\left(\left|\frac{\eta_0}{4\eta}\right|e^{t/\delta}\right) + 20\log\left(e^{t/\delta}\right) + 20\log\left(\left[1-e^{-j2t/\delta}e^{-j2t/\delta}\right]\right) \tag{2-29}$$

$$SE_{dB} = R_{dB} + A_{dB} + M_{dB} \tag{2-30}$$

Therefore, the SE of the material can be determined at any frequency, by using equation (2-31).

The source is one of the most important parameters to determine the Shielding Effectiveness of an enclosure. Distinction must be made between far fields (plane wave source) and near fields (electrical, magnetic source). In this document, we will generally study the effect of near field sources since the source of emissions in an enclosure is the electronic board inside that is located in the near field of the box wall. The main difference is the behavior of the E fields that will no longer vary as 1/r but as $1/r^2$. Previous equations will then have to be modified to reflect the change due to this type of source. [7][10]

The absorption loss, however, will not vary due to the source proximity and can be approximated by the following formula [7][18]:

$$A_{dB} = 131.4t\sqrt{f\mu_r\sigma_r} \qquad (2\text{-}31)$$

The reflection loss will be changed. For an electrical source, R_e (dB) is given by [7][18]:

$$R_{e,dB} = 322 + 10\log\left(\frac{\sigma_r}{\mu_r f^3 r^2}\right) \qquad (2\text{-}32)$$

There is a more simple method for determining SE of intrinsic material; it is by using Nomographs [7]. This tool is often used instead of the previous equations to determine SE of a material, since for the mechanical engineer, the solution is obtained in a more straightforward way, without any big mathematical manipulations.

CHAPTER 3

THEORETICAL ESTIMATE OF SHIELDING EFFECTIVENESS

Radiated emissions from cavities, at frequencies below cavity-mode resonance, have been investigated experimentally and numerically in the past. Recently, work has been done [2][3][12][14][19] on estimating the electrical field strength with help of numerical simulations, measurements, and equivalence principles, to estimate the radiation from apertures. The effect of aperture dimensions on Shielding Effectiveness and the method to estimate the Q of an enclosure at resonance, have also been studied [3][12][13][19].

However, all those past studies used extensive theoretical calculations, complicated experimental set-ups and numerical analysis, which are very detailed and cannot be practice in today's industry. A simple and practical approach is needed to guide the EMC design engineer.

In this thesis, a simple expression for SE estimation, for small enclosures, has been developed from published formulae and will be presented in this chapter. The SE estimate includes all useful parameters for the design:

length of slots or apertures, frequency, Q and the enclosure volume.

In the design process, where little is known, and mechanical data starting points are unknown, this formula can be used as an initial assessment of the Shielding Effectiveness. The estimate can also be used to guide airflow aperture design, gasketing and to verify interior partitioning and PCB population effect on the enclosure SE.

3.1 Simple Enclosure Model.

To test the formula predictions against measurements and calculations, a closed box test case with and without a PCB is used. A rectangular aluminum enclosure was chosen, arbitrarily, to study the attenuation as a function of the frequency. This "case study" serves to assess the accuracy of the "SE estimate" against measurements and against numerical simulations.

A rectangular aluminum box, of 188.8 mm. by 188.8 mm. by 63.5 mm. is used. A round 12.7 mm. diameter aperture is present in the middle of the cover, with the purpose of controlling the leakage point. It has been previously proven experimentally and numerically, that electrically small rectangular and round apertures, of same areas, have approximately the same radiated emission level [15][3][19]. A Mechanical schematic of the simple model enclosure is presented in Appendix B. A Photo of the physical enclosure is also presented below.

Figure 3-1: Simple Enclosure with leakage hole.

3.2 SE Theoretical Estimation Formula

3.2.1 Small Hole Fields

Making the assumption that the major leaking point of our enclosure is the round hole, the development of a SE estimation can then be simplified. The Bethe small hole coupling theory, relates the far-field radiation from a small hole as [3][15][19] to the magnetic field.

$$\left|E_{far}\right| = 120\pi \frac{2\omega^2 a^3 |H|}{3\pi c^2 R} \tag{3-1}$$

where $2\pi f = \omega$, is the angular frequency, a is the radius of the hole, c is the speed of light (3×10^8 m/s), R is the distance between the source and the observation point (for our study: 1 meter) and H, the tangential magnetic field across the aperture in the absence of the hole.

The Bethe small hole theory can also be expressed as a radiating magnetic dipole $\vec{M}$, along the plane of the hole and an electric dipole $\vec{P}$, along the normal direction of the hole.

The electric and magnetic dipoles are related to the short circuit magnetic field ($\vec{H}_0$) in the plane of the hole and the normal short-circuit electric field ($\vec{E}_0$) as follows [3][19];

$$\vec{M} = P_m \vec{H}_0 \tag{3-2}$$

$$\vec{P} = P_e \vec{E}_0 \tag{3-3}$$

The electrical dipole has no effect on the strength of the far electrical field in front of the aperture panels. The magnetic polarization for a round hole can be expressed as [11][16][19]

$$P_m = \frac{4}{3} a^3 \tag{3-4}$$

3.2.2 Cavity Fields.

The interior fields for a TM_z (mnp) mode in an ideal rectangular cavity are [17] [3][19]

$$E_x = A_{mnp} \frac{j}{\omega \mu \varepsilon} \beta_x \beta_z \cos(\beta_x x) \sin(\beta_y y) \sin(\beta_z z) \tag{3-5}$$

$$E_y = A_{mnp} \frac{j}{\omega\mu\varepsilon} \beta_y \beta_z \sin(\beta_x x)\cos(\beta_y y)\sin(\beta_z z) \tag{3-6}$$

$$E_z = -A_{mnp} \frac{j}{\omega\mu\varepsilon} (-\beta_z^{\,2} + \beta^2)\sin(\beta_x x)\sin(\beta_y y)\cos(\beta_z z) \tag{3-7}$$

$$H_x = A_{mnp} \frac{\beta_y}{\mu_0} \sin(\beta_x x)\cos(\beta_y y)\cos(\beta_z z) \tag{3-8}$$

$$H_y = -A_{mnp} \frac{\beta_x}{\mu_0} \cos(\beta_x x)\sin(\beta_y y)\cos(\beta_z z) \tag{3-9}$$

$$H_z = 0 \tag{3-10}$$

Where $\beta_x = \frac{m\pi}{a}$, $\beta_y = \frac{m\pi}{b}$, $\beta_z = \frac{m\pi}{c}$ and A_{mnp} is the vector potential constant determined, by the source. To determine A_{mnp}, we need to relate the total energy stored in the enclosure to the TM_z field, trough the magnetic energy W_μ as follows [17][19]:

$$W = 2W_\mu = \frac{2\mu_0}{4}\int H^2 dv = \frac{\mu_0}{2}\int_0^a \int_0^b \int_0^c \left(H_x^2 + H_y^2\right) dx dy dz \tag{3-11}$$

$$W = A_{mnp}^2 \frac{V}{8\mu_0}\left(\beta_x^2 + \beta_y^2\right) = \frac{P_d Q}{\omega} \tag{3-12}$$

From Equation 3-12, A_{mnp} can be found as

$$A_{mnp} = \sqrt{\left[\frac{8\mu_0 P_d Q}{V\omega(\beta_y^2 + \beta_x^2)}\right]} \tag{3-13}$$

where V, is the volume of the enclosure, P_d is the power delivered to the enclosure and Q is the ratio of the time-averaged energy stored in the cavity to the dissipated power. The value of Q has been related to populated printed circuit board (PCB) in other studies. [12][11][3][19] Q should vary from 10 to 50; ten being a fully populated PCB and fifty a simple PCB.

3.2.3 Small Field to Cavity Relationship.

Assuming the hole center is at the origin, then by using Equation (3-8) and Equation (3-12) the magnetic field on the aperture face is [3][19]

$$H_z \frac{A_{mnp}\beta_y}{\mu_0} = \sqrt{\left[\frac{8\mu_0 P_0 Q}{n_g V\omega(\frac{\beta_x^2}{\beta_y^2}+1)}\right]} \tag{3-14}$$

where V is the volume of the enclosure. Using Equation (3-1) and substituting Equation (3-14) the electrical far field can be expressed as follows [3][19]:

$$\left|E_{far}\right| = \frac{22.3(2\pi)^{\frac{3}{2}}a^3}{c^2 R}\sqrt{\left[\frac{P_0 Q}{n_g u_0 V\omega(\frac{\beta_x^2}{\beta_y^2}+1)}\right]} \tag{3-15}$$

where $P_0 = \frac{V_s^2}{2R_s}$, stands for full power. It is assumed that all the available power is delivered to the enclosure. V_s, is the amplitude of the noise source voltage, which has been arbitrarily chosen to be 1mV. for this study and R_s, is the noise resistance. Assuming β_x and β_y are very close modes,

Equation (3-15) simplified as [3][19]:

$$|E_{far}| = \frac{31.6(2\pi)^{\frac{3}{2}} V_s a^3 f^{\frac{3}{2}}}{\sqrt{\mu_0 c^2 R}} \sqrt{\frac{Q}{R_s V}} \qquad (3\text{-}16)$$

Once more, for our purpose, R = 1m. (far-field see Chapter 4), the noise source voltage is fixed to 1mV, a noise source impedance at 50 ohms. We can obtain a SE approximation using the assumption that, the free-space field is radiating from a small linear dipole. The Shielding Effectiveness formula obtained, is for the worst-case scenario, where full power is delivered to the enclosure [3][19]:

$$SE_{dB} = 1.2\times10^{12} \frac{\sqrt{V/Q}}{a^3 f^{\frac{3}{2}}} \qquad (3\text{-}17)$$

where V, is the volume of the enclosure, f the frequency, a is the radius of the hole and Q, the Quality factor ranging from 10-50. [3] [19]. Equation 3-17 is also calculated using the radiated power from the short dipole as available power. From this equation it is important to visualize the effect of Q, V and a over SE. The three figures below show the sensitivity of SE for the above parameters. V, Q and a play an important role in estimating SE. The most sensitive parameter is the radius of the aperture, which makes the attenuation degrade at a much bigger rate from Figure 3-3. Q is the second most

important factor to which designer should pay attention to optimize the shielding. Partitioning may be a good option to decrease Q and increase the Attenuation as in Figure 3-2. The volume may also be changed, however, outside dimension may be a constraint for mechanical reasons and cost. From Figure 3-4, the volume changed the Attenuation a little bit less than Q.

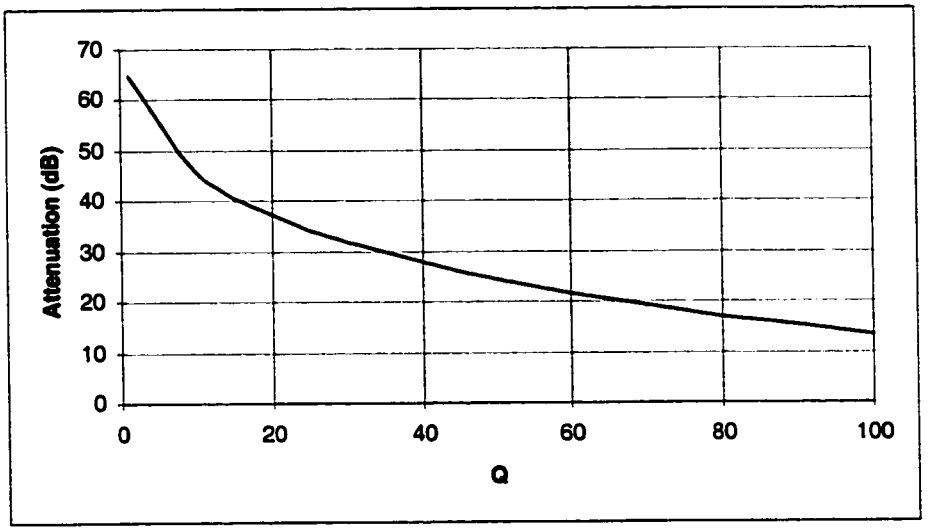

Figure 3-2: Attenuation function of the parameter Q

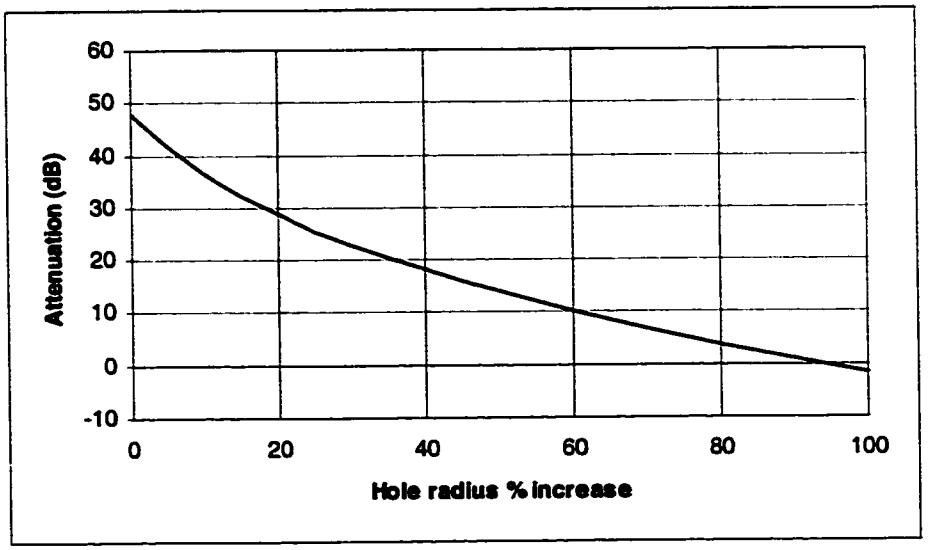

Figure 3-3: Attenuation function of the % increase of the radius of the hole

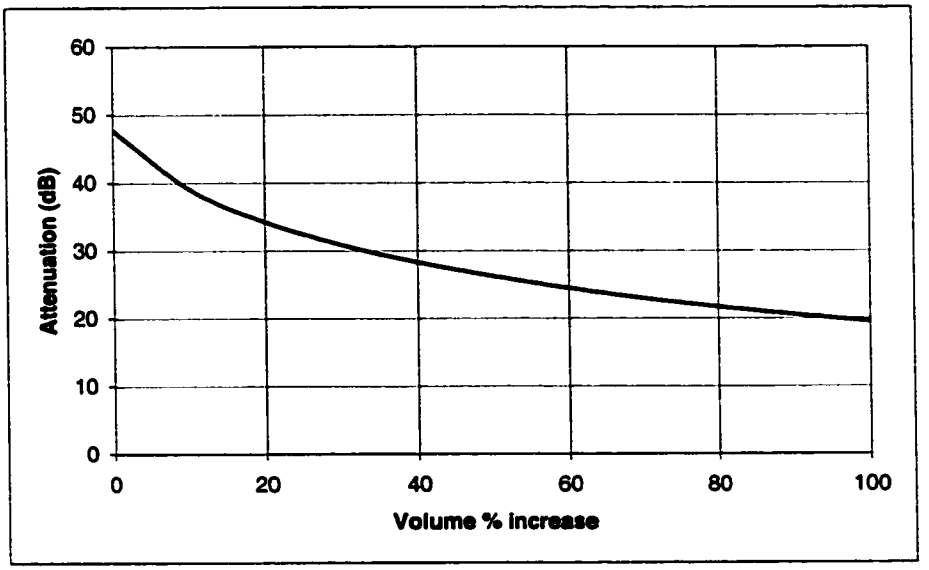

Figure 3-4: Attenuation function of the % Volume increase of the enclosure

3.3 Resonance.

Knowing the resonance frequencies of an enclosure can be helpful to suppress the emissions. The engineer can adjust his design in consequence by adding lossy material or by breaking the cavity in multiple sections.

The resonant frequency, of the cavity, can be determined using formulas from literature [3][16][17]. The following expression is basic to all rectangular cavities:

$$(f_r)_{mnp}^{TE} = \frac{1}{2\pi\sqrt{\varepsilon\mu}}\sqrt{\left(\frac{m\pi}{a}\right)^2 + \left(\frac{n\pi}{b}\right)^2 + \left(\frac{p\pi}{c}\right)^2} \qquad (3\text{-}18)$$

where $m = 0,1,2,\ldots; n = 0,1,2,\ldots; p = 1,2,3,\ldots$ and $m = n \neq 0$.

Determining the Q of an empty enclosure is also possible and helpful at the beginning of a design to support a partitioning option. To determine the Q of an ideal rectangular enclosure, the following formula can be used; were R_s is the surface resistance of the enclosure [17]:

$$(Q_{mnp}) = \frac{\pi\eta}{2R_s}\left[\frac{b(a^2+c^2)^{3/2}}{ac(a^2+c^2)+2b(a^3+c^3)}\right] \qquad (3\text{-}19)$$

$$R_s = \sqrt{\frac{\pi f_r \mu}{\sigma}} \quad \text{(ohms)} \qquad (3\text{-}20)$$

Values of Q and resonant frequency for our simple model are presented in Table 3-1. At each TE excitation mode the resonant frequency and Q have been evaluated using Equation (3-19) and Equation (3-20). The first resonant frequency and fundamental is the TE_{101} Mode at 1159.19 MHz.

Table 3-1: Simple empty enclosure model Q and resonant frequency values.

Mode	f_r (MHz)	Q
TE_{101}	1159.19	15632.29
TE_{011}	2500.37	10643.82
TE_{111}	2631.30	10375.64
TE_{102}	1832.84	12431.90
TE_{201}	1832.84	12431.90
TE_{021}	4794.99	7686.11
TE_{012}	2875.32	9925.61
TE_{112}	2989.87	9733.61
TE_{121}	4864.54	7630.96
TE_{211}	2989.87	9733.61
TE_{103}	2592.03	10453.94
TE_{301}	2592.03	10453.94
TE_{031}	7133.86	6301.41
TE_{013}	3409.81	9114.55
TE_{113}	3506.94	8987.44
TE_{131}	7180.80	6280.78
TE_{311}	3506.94	8987.44
TE_{104}	3379.59	9155.20
TE_{401}	3379.59	9155.20
TE_{041}	9484.30	5465.09

Note: $\sigma = 3.96E-7 \quad S/m.$

3.4 Theoretical analysis of the simple enclosure

For the simple enclosure, results of theoretical SE estimations using Equation (3-17) are presented, below, for the frequency range of 622 MHz to 10 GHz in the plot below for two different Q (Q=10 and Q=50)) and $\sigma = 3.96E-7 \quad S/m$.

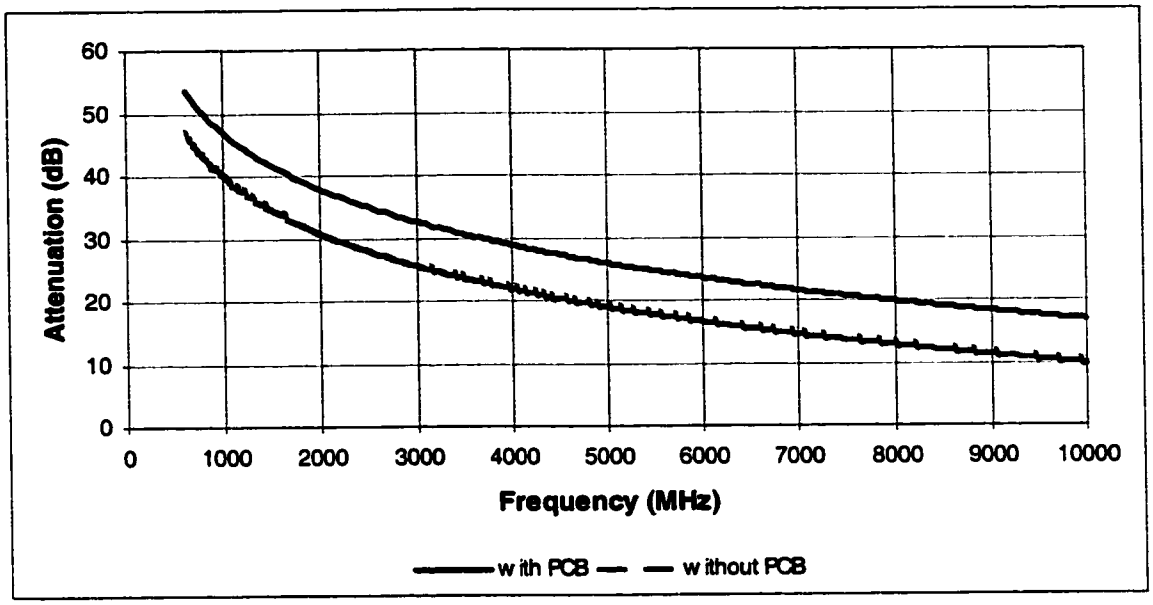

Figure 3-5: SE theoretical estimation

Figure 3-5 above, shows that the Shielding Effectiveness of the enclosure is very low, after 4000 MHz: 15 dB (average). The difference between both case studies is 6.9 dB, which indicated that cavity partitioning help the shielding, by increasing the attenuation of the enclosure. Moreover, the case study with a PCB provided more then 20 dB of shielding up to 8700 MHz. The test case without PCB provided more then 20 dB of shielding up to 5000 MHz. Attenuation for the case study without a PCB is lower than with a PCB. This follows Balanis and Krauss electromagnetic books [24] and supports the fact that Q is normally added in the same manner as for resistances in parallel circuits. Hence, partitioning is then a very good option to increase shielding in our case.

Q of our empty enclosure is in the 1000 to 10000 range depending on the mode.

The lowest resonant frequency is around 1.159 GHz. This is very high and can be pushed much higher with partitioning or the presence of a populated PCB.

3.5 Discussion on Theoretical SE Estimation.

Theoretical analysis is very useful at the beginning of the design process, when project architecture takes form. This kind of analysis removes a certain amount of "ballpark" guessing and gives better directions to the project. At the beginning of a project, pressure is on the EMC engineer to give appreciable value for dimensions, which are mostly gross estimates. Using an theoretical estimation is limited, however, any designer can easily use it in a matter of seconds. Simplifications of a model need to be made in order to use the theoretical analysis method. Generally, the designers use the biggest aperture as the main leakage point to predict the SE of an enclosure. This assumption is far from being ideal; nevertheless, it is still the best approach at this stage. Other developed formulas for multiple holes and rectangular apertures have been developed and are presented in Appendix C. The most useful SE approximation and the mostly used is the honeycomb SE estimation formula. One of the biggest challenges of EMC is the trade off between thermal design and EMI. The thermal engineer wants BIG holes and EMC engineer wants No hole! To overcome this dilemma, designers use Honeycombs (wave guides) perforated vent panels. These allow airflow without too much constraint and provide a certain amount of shielding. The formula for honeycomb SE estimation is presented in Appendix C.

The SE estimate given in Equation (3-17) above, based on Bethe small hole theory, gives a good first approximation. Fast results can be obtained and optimization of some dimensions can be made. This method should not be used past a certain stage in the

design process. It is a good estimation method for very simple or basic architectural design. However, when the shield becomes complex, it can't take into account all the parameters in its theoretical formulas. More study, on source voltage and impedance, should be done to improve this estimation method.

The use of the theoretical analysis is most successful when used in conjunction with an experimental estimation. The experienced engineer will certainly do better than a beginner, using this kind of estimation. In view of the fact that, at a certain level, it involves simplification of model parameters and extrapolation of SE estimation values to reflect secondary leakage points and gaskets.

An experimental protocol to estimate SE of a small enclosure will be introduced in the next chapter, following the same methodology as for the theoretical analysis.

CHAPTER 4

MEASUREMENT OF SHIELDING EFFECTIVENESS

Experimental corroboration is one of the most important parts of a design process. With this kind of experiment, an engineer can validate a design using a realistic approach. However, to be able to do such estimated measurements, a physical representation of the final unit must be provided. The Aluminum box presented in Section 3.1, will be used for comparing experimental results of SE estimations against the empirical and numerical simulation analysis, in this thesis.

Numerous SE measurement methods have been published for small enclosures [2][9][14]. Most of them need special tools and handling, and , are only applicable to a specific experiment. The method used in this study is based on measurement of radiated emissions, which is then related to Shielding Effectiveness by the reciprocity theorem presented in Chapter 2. [18][5] The measured transmitted field (radiated field from the box) by reciprocity with the SE definition, where a received plane-wave is measured, should be the same.

4.1 Enclosure Under Test Description.

The "test case" consists of the aluminum box described in Appendix B with a 12.7 mm. diameter hole on the cover. It is assumed that the only coupling between the interior and exterior is via the hole. That is, the attenuation of the aluminum walls is so large that the fields leaking directly through the walls are negligible [7]; Figure 4-1 shows attenuation curves for different thickness of aluminum 6061 using Equation (2-33).

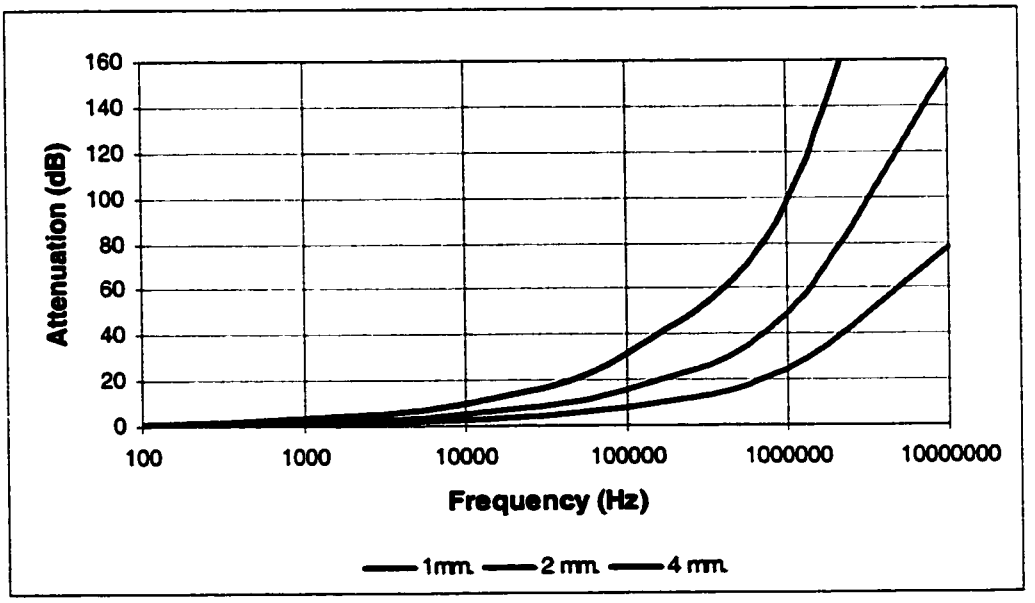

Figure 4-1: Attenuation for Aluminum 6061.

To eliminate possible leakage from the seams of the cover, copper tape was applied around the cover to the rest of the enclosure to provide a perfect seal. Figure 4-2 shows details of copper seal and enclosure, ready for testing. The noise source center position was arbitrarily chosen inside the enclosure. One can push the study further by

displacing the noise source inside the enclosure for variance. A note should be made that The noise source is not grounded to the enclosure.

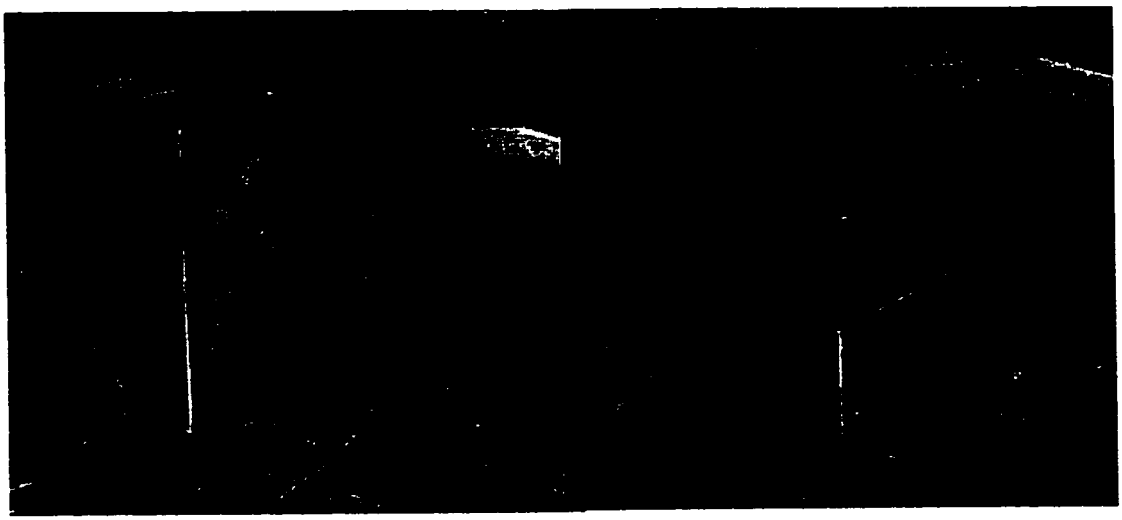

Figure 4-2: Enclosure under test with copper

The battery power noise source consisted of a VCO and a regulator mounted on a PCB with 2 loop antennas. The noise source is 5 cm. by 4 cm. by 2 cm. (see appendix F for details on noise source). It is mounted in a plastic box cover. Figure 4-3 presents a close view of the battery noise source. [5]

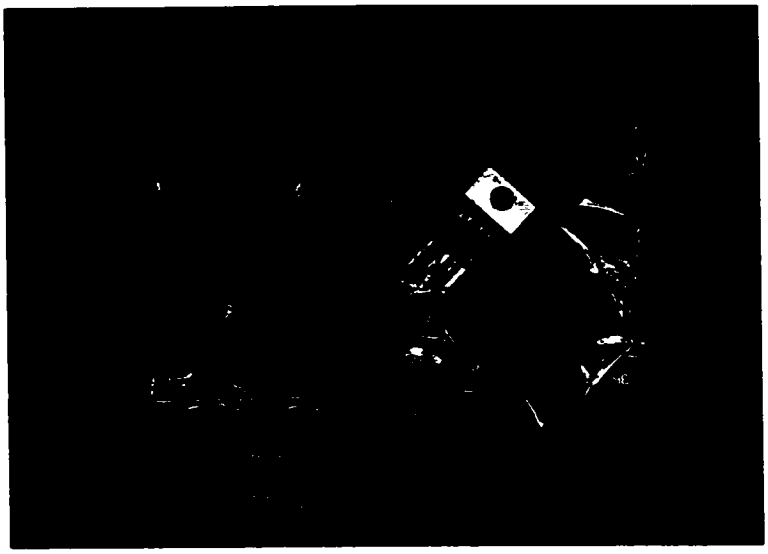

Figure 4-3: Battery powered noise source, close view.

The VCO is changeable, making frequency selection more available. Each crystal limits measurement to its fundamental and harmonics. For this Thesis, a 622.08 MHz ECL clock is used. The frequency range covered is 622.08 MHz to almost 10 GHz. [5]

Two test cases have been investigated. The first test case is the empty aluminum enclosure, and the second case is the aluminum enclosure with the copper board inside. In fact, the first case is the box with the noise source and the second case is the box with the noise source and copper board. Figure 4-4 presents the first test case without PCB, and the second with PCB. The copper PCB filler is used to simulate the presence of a real PCB board. The PCB is located 2 cm. from the inside bottom of the enclosure and it is not grounded to the chassis. The noise source is located in the middle of the PCB inside the enclosure. The PCB dimensions are 160 mm. by 160 mm. by 2 mm..

Figure 4-4: Open enclosure under test: a) test case without PCB, b) test case with PCB 2 cm from the bottom of the enclosure.

4.2 List of the Equipments.

The following table lists all necessary test equipment used for attenuation measurements. Figure 4-5 below presents a diagram of equipments connections for our experimental measurements of Table 4-1. Figure 4-8 in section 4.4 relates test equipment to setup for measurements.

Table 4-1: Test equipments

Description	Model Number	Serial Number
Spectrum Analyzer	HP 8593E	3308A00587
Coax cable	SUHNER SUCOFLEX 100	N/A
Horn Antenna	EMCO 3115	9711-5314
Antenna Tripod	EMCO	N/A
Turn Table	C-MAC	N/A
Turn Table Controller	EMCO	761332-01
Amplifier	LNA 1Ghz-18Ghz	BNR A5
GPIB Cable	HP GPIB SHIELDED CABLE	N/A
Noise Source	001	001
Computer	THINKPAD A21m IBM	78-KVX7

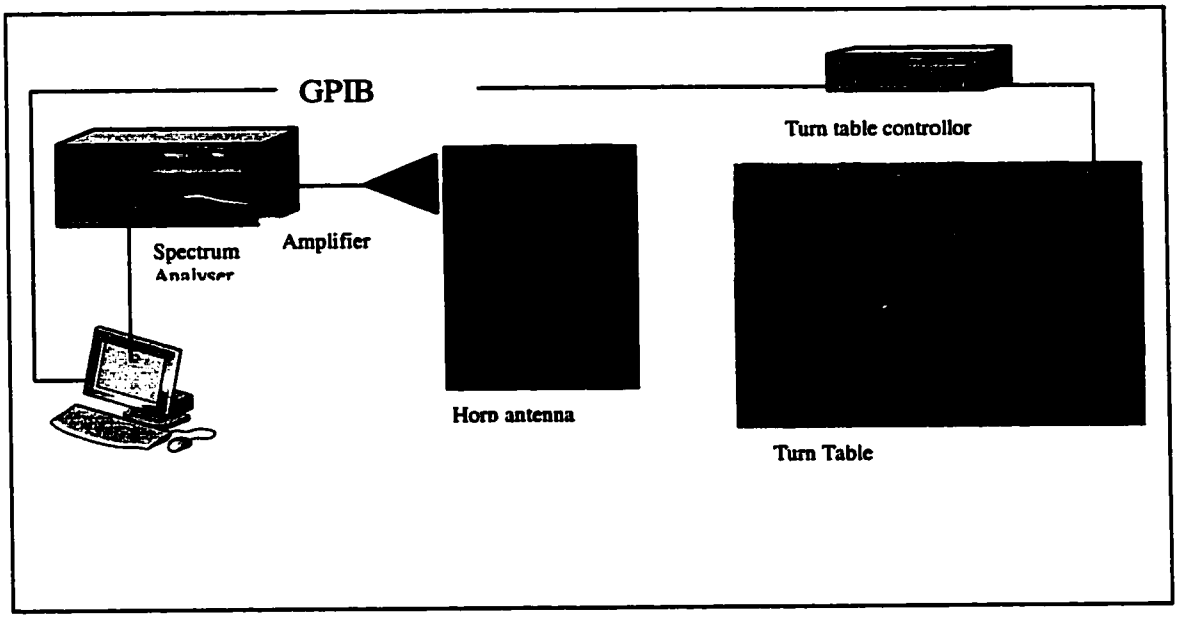

Figure 4-5: Equipment set up diagram

4.3 Facility

A 3 m. Semi-Anechoic chamber, ferrites lined with absorbing cones on the walls and ceiling at C-MAC Engineering was used. The chamber is ANSI C63.4 compliant (see Appendix D for statement). [20] An open area test site (OATS) can also be used for testing. However, in our case, luxury and availability of an ambient free chamber (AFC) is possible and suppresses any ambient from our data shielded rooms, which is not recommended because the resonance can give faulty results.

Figure 4-6 shows the 3 m. Semi-Anechoic chamber with absorbing cones, ferrites tiles and turntable setup. The ferrite tiles and cones are present to suppress any reflections

from the walls. Ferrites are normally composed of carbon material, and cones are Styrofoam covered or injected with carbon filler. [5]

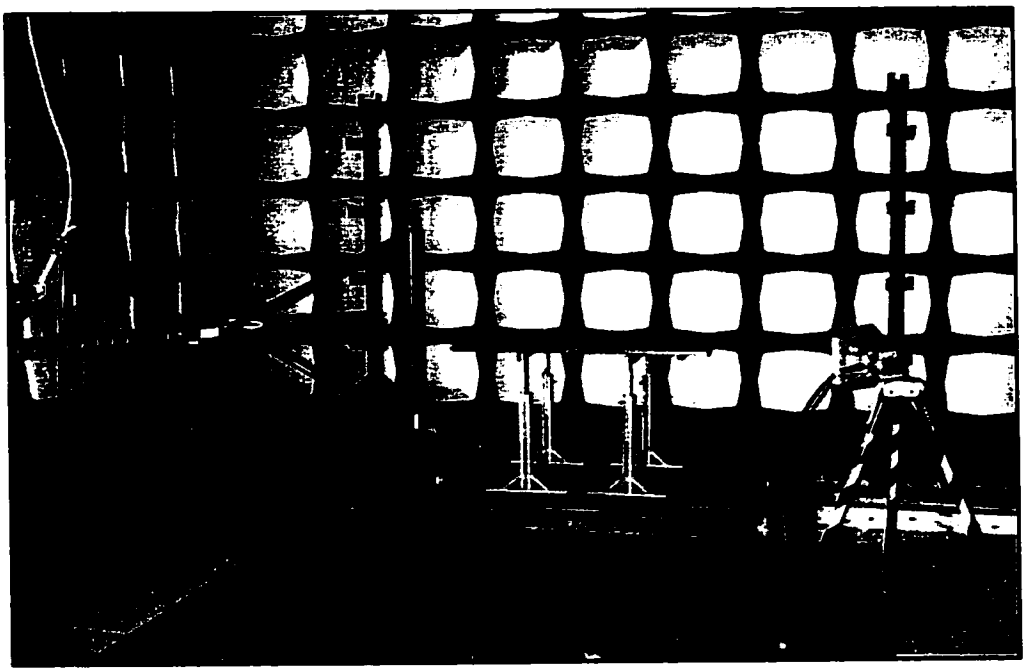

Figure 4-6: The 3 m. Semi-Anechoic chamber

4.3.1 Environmental Conditions.

Room temperature and humidity are monitored for good manufacturing practice. A relative humidity of 30% and a room temperature of 20 degree Celsius are recommended.

4.4 Detailed Procedures.

There are two main procedures that are involved in SE measurements [5][14]:

1. the characterization of the free space electronic noises, and
2. the testing of the enclosure itself.

In this study noise in free space is defined as the bare noise source circuit on the experimental table.

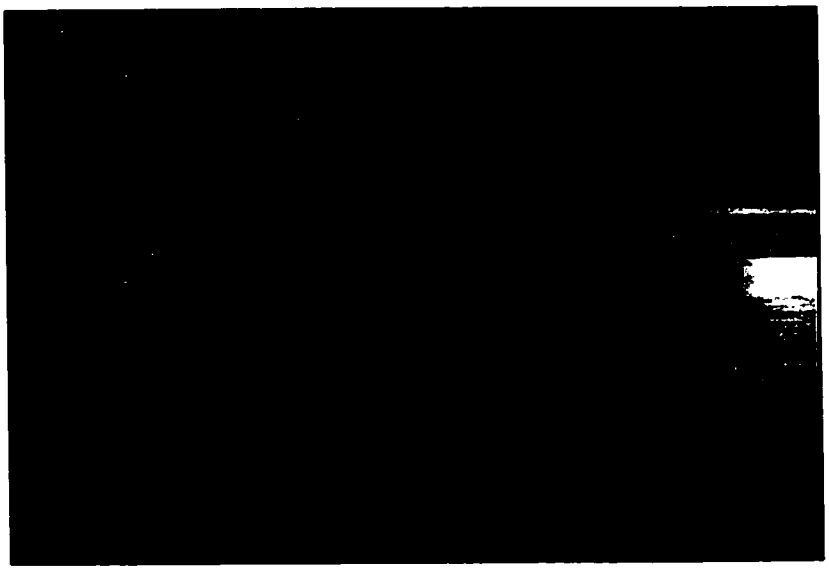

Figure 4-7: Noise source on wood table ready for measurements.

SE is based on a difference between two signals. Therefore, no antenna or amplifier factors need to be used. However, it is important that the experimental apparatus, including antennas, amplifiers and distances used, remain constant throughout the entire test procedure (Enclosure and free space characterization). The Shielding Effectiveness experimental setup is presented in Figure 4-8. The antenna is located 1 meter from the closest edge of the EUT and 1 meter above the ground plane on a wood table.

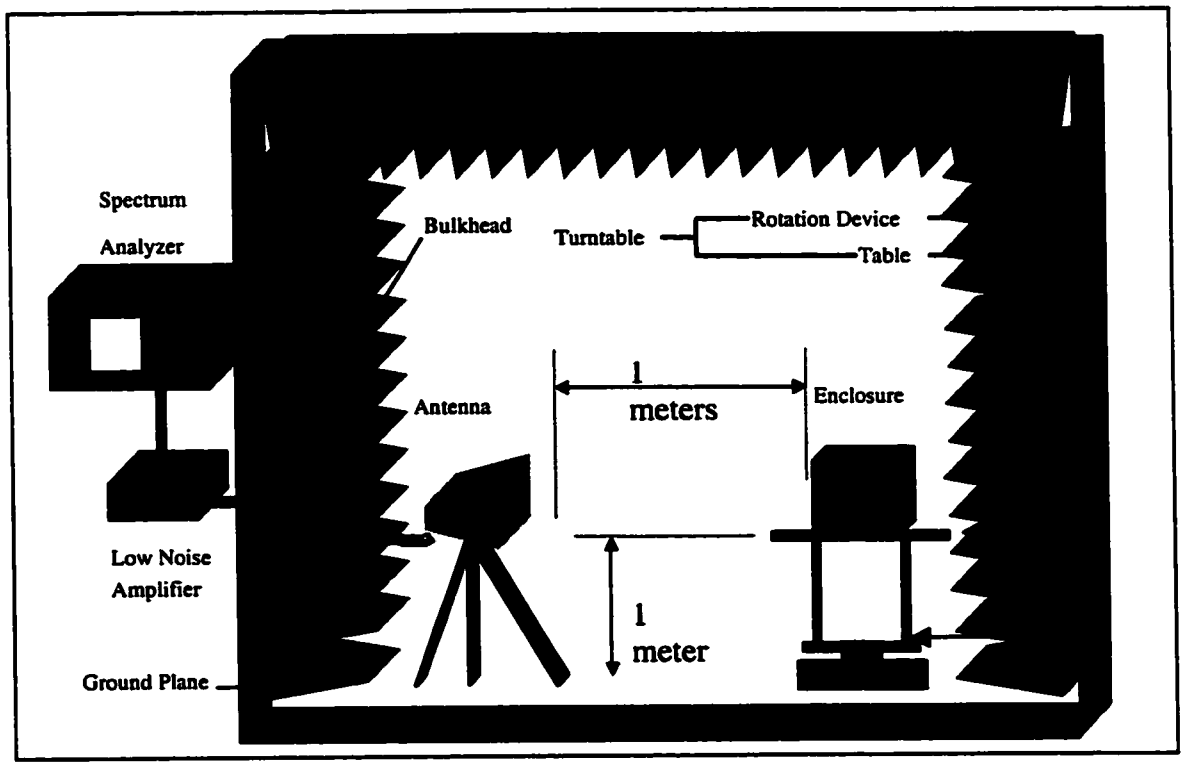

Figure 4-8: Experimental setup inside a 3 m. ambient free chamber. [5]

At 1 m. the receiving antenna is considered to be in the far field. This occurs at $\frac{2D^2}{\lambda}$ in m. approximately, where λ is the wavelength of the electromagnetic wave and D the largest dimension of the enclosure [4]. For our purpose, the lower frequency of interest is 622.08 MHz, making the far field position at approximately 0.82 meters. A horn antenna is used as the transducer for our experiment. The choice of antenna is based on the frequency range to cover. The horn antenna and experimental setup are presented in appendix E.

4.1 Characterization Free Space Electronic Noise.

The battery noise source must be characterized in free space for each session of SE testing of an enclosure or, after any set-up changes. The Battery Noise Source is placed inside the testing facility at the approximate position that it will be placed in the aluminum box and turned on. The turntable is then fully rotated (360 degrees) to determine its maximum peak emission level with the spectrum analyzer. Maximum peak emission level of each harmonic of the noise source is measure only. We are limited to discrete frequency due to the ECL clock.

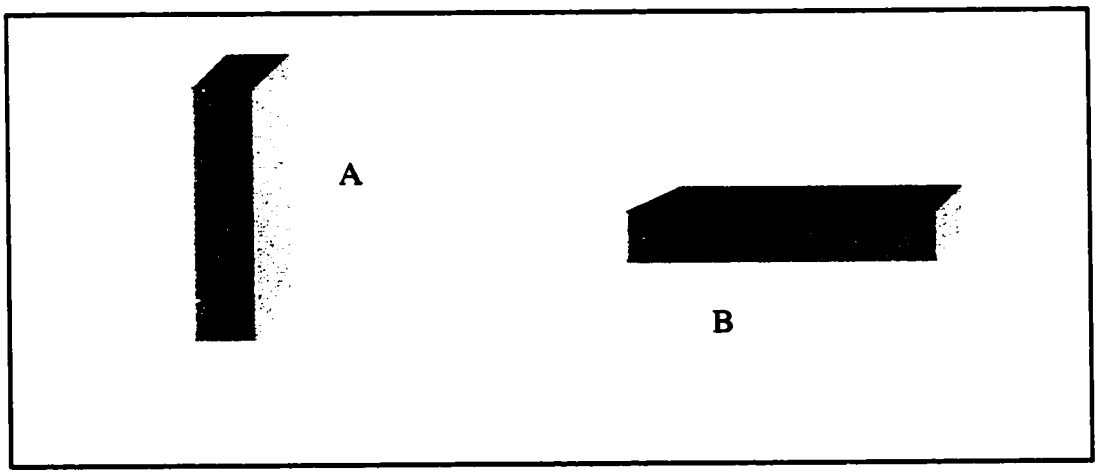

Figure 4-9: Polarization of the noise source in free space A) Vertical B) Horizontal. [5]

Table 4-2: Noise source possible permutation. [5]

	Antenna	Noise source
1	Vertical	Horizontal
2	Vertical	Vertical
3	Horizontal	Horizontal
4	Horizontal	Vertical

Actual Free-Space noise source set-up is presented in Figure 4-10.

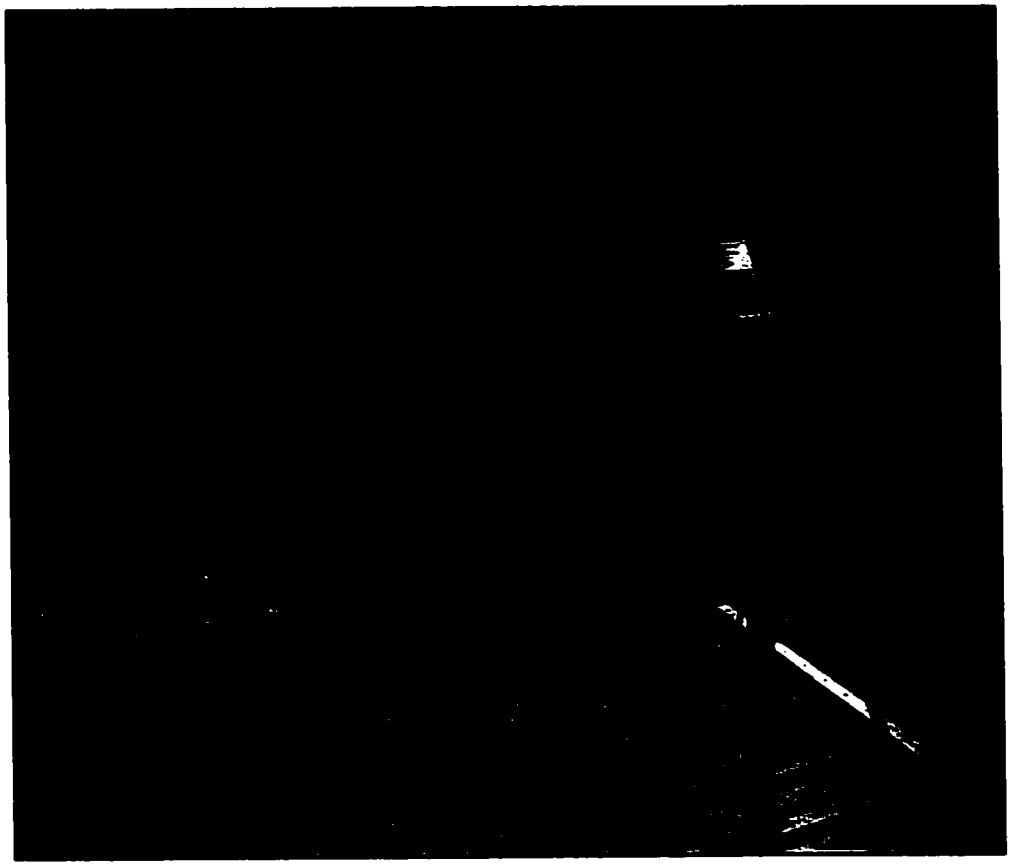

Figure 4-10: Free Space Noise source characterization setup.

The maximum peak emission level of each harmonic from all four combinations is the final value that is used in the calculations for shielding effectiveness, in order to assume the worst case shielding. The four orientations of Table 4-2 and Figure 4-9 are used, to make sure that the largest field strength emitted by the box is measured, in each case the turntable is rotated through 360 degrees. Ideally the measurement of the full volumetric radiation patterns of the box, i.e. measurement of the magnitude and phase, and over the radiating sphere by measuring the patterns, e.g.: = 0,25, 37, 45, 84, 90, 96,..., 135, 150, 180 degrees, will be more precise. However, the procedure is too expensive and time consuming, so measurement of some "principal plane" cuts as in

Table 4-2 give good sampling and chance to find the largest sample field values. The four orientations of Table 4-2 do not measure the largest field. The field is elliptically polarized and it is needed to find the orientation that is "parallel" to the big axis of the polarization ellipse to get maximum emission. This can be calculated if the magnitudes and phases of the two field components are measured, however, this would require a "vector" network analyzer, which is expensive.

It is a good practice to measure the dynamic range of the noise source at this stage, to make sure that there is enough resolution everywhere in the frequency range. To accomplish this task, the subtraction of the noise source emission level and the noise floor measurement is done. From experience, a minimum of 20 dB of dynamic range is needed.

For the experimental estimation, it is desirable to develop an equation for attenuation in dB uV/m. terms, since, radiated emission measurements are done on a spectrum analyzer in this unit. Allowing V_i/m. to represent the free space field strength (no enclosure) and V_t/m., to represent the attenuated field strength coming out of the enclosure (both in uV/m):

The difference of V_i and V_t gives the attenuation of the enclosure, which by the reciprocity theorem equal to the SE

$$SE = 20\log V_i - 20\log V_t \tag{4-1}$$

$$SE = A - B \text{ dB} \tag{4-2}$$

where *A* is the field strength as measured on the spectrum analyzer in dBuV/m [5], without the enclosure, and *B*, is the attenuated field strength as measured on the spectrum analyzer with enclosure, also in dBuV/m..

4.4.1.2 Tests Results for Free Space Noise.

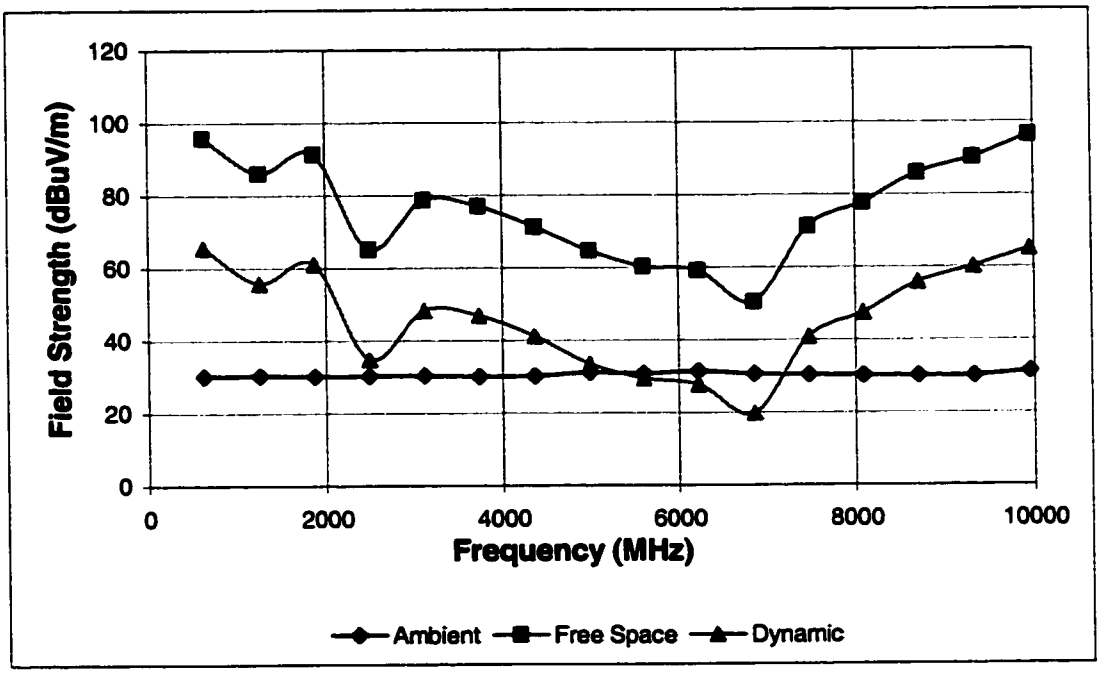

Figure 4-11: Free space noise characterization, ambient noise, and dynamic range.

The ambient field strength (Emission present in the empty chamber) of Figure 4-11 shows a typical 32 dB uV/m. noise floor for a shielded room. Variation of the field strength is minimal: +/-1 dBuV/m. There is no ambient emission that can be added in our results. The dynamic range of the experiment shows a minimum of 20 dBuV/m at 6800 MHz which is just enough for the experiment. The "free space" curve is the measurement of the maximum field radiated by the noise source in the four

orientations of Table 4-2 with the turntable rotated 360 degrees. The "dynamic" curve is the "free space" curve minus the noise floor curve. For example, the "dynamic" curve at 1000 MHZ is 90 dB minus 32 dB equals 58 dB. Dynamic range gives a relative idea of noise level radiated against the room ambient.

Free space noise characterization shows a minimum of 50 dB μ V/m. and a maximum of 90 dB μ V/m. of field strength. Free space noise characterization is the noise source radiated emission measurement, which is used in the enclosure attenuation calculation. Ideally, a flat response will be better over our frequency range. However, antenna, amplifier and noise source "power" introduce variances.

4.4.2 Enclosure Characterization.

After the battery noise source has been characterized in free space, Shielding Effectiveness testing of the enclosure can be done. The battery noise source is placed as close as possible to the center of the Aluminum box as in Figure 4-3. The procedure below must be performed for every combination stated in Table 4-3 and for the Aluminum enclosure with and without the PCB. In each case the turntable is rotated 360 degrees. [5]

Table 4-3: EUT/noise source possible permutations. [5]

	Antenna	EUT/Noise source
1	Vertical	Horizontal
2	Vertical	Vertical
3	Horizontal	Horizontal
4	Horizontal	Vertical

The maximum sample emission level of each harmonics, from all four combinations, is the final value that is used in the calculations of Shielded Effectiveness in order to assume a worst case shielding. More combinations are possible, but from experience, the above four always radiate higher emission level then other combinations. Note that the field is elliptically polarized and it is needed to find the orientation that is "parallel" to the big axis of the polarization ellipse to get maximum emission, so the four combinations in Table 4-3 are good samples of the Maximum field strength emission. This test must be repeated for each EUT configuration, Table 4-3, and rotated 360 degrees.

4.4.2.1 Test Results of Enclosure Characterization.

Results for the enclosure characterization are summarized in Table 4-3 and Table 4-4 for the enclosure with PCB and without PCB.

Table 4-3: Enclosure characterization results without PCB.

Frequency (MHz)	Max free space noise (dBuV/m)	Max enclosure noise (dBuV/m)	Shielding effectiveness (dBuV/m)
622.08	95.82	45.4	50.42
1244.08	86.08	49.32	36.76
1866.08	91.34	55.06	36.28
2488.08	65.13	35.83	29.3
3110.08	78.7	50.26	28.44
3732.08	76.98	54.54	22.44
4354.08	71.32	59.93	11.39
4976.08	64.71	57.13	7.58
5598.08	60.3	48.6	11.7
6220.08	59.13	43.2	15.93
6842.08	50.44	36.4	14.04
7464.08	71.3	56.3	15
8086.08	77.74	64.3	13.44
8708.08	85.92	72.1	13.82
9330.08	90.23	77.5	12.73
9952.08	96.36	84.3	12.06

Table 4-4: Enclosure characterization results with PCB.

Frequency (MHz)	Max free space noise (dB uV/m)	Max enclosure noise (dBuV/m)	Shielding effectiveness (dBuV/m)
622.08	95.82	39.66	56.16
1244.08	86.08	36.6	49.48
1866.08	91.34	48.93	42.41
2488.08	65.13	31.2	33.93
3110.08	78.7	46.5	32.2
3732.08	76.98	51.4	25.58
4354.08	71.32	52.4	18.92
4976.08	64.71	47.11	17.6
5598.08	60.3	43.08	17.22
6220.08	59.13	40.23	18.9
6842.08	50.44	32.84	17.6
7464.08	71.3	53.1	18.2
8086.08	77.74	60.31	17.43
8708.08	85.92	68.8	17.12
9330.08	90.23	73	17.23
9952.08	96.36	83.7	12.66

The following Figure shows both test case results. In both cases, the curve patterns are similar to the "Free space" and "Dynamic range". The signal is lower than in free space, which is expected. Emission plots can be very tempting to compare to the standard limits. Such comparison is impossible to do since transducers should be accounted for in the calculation.

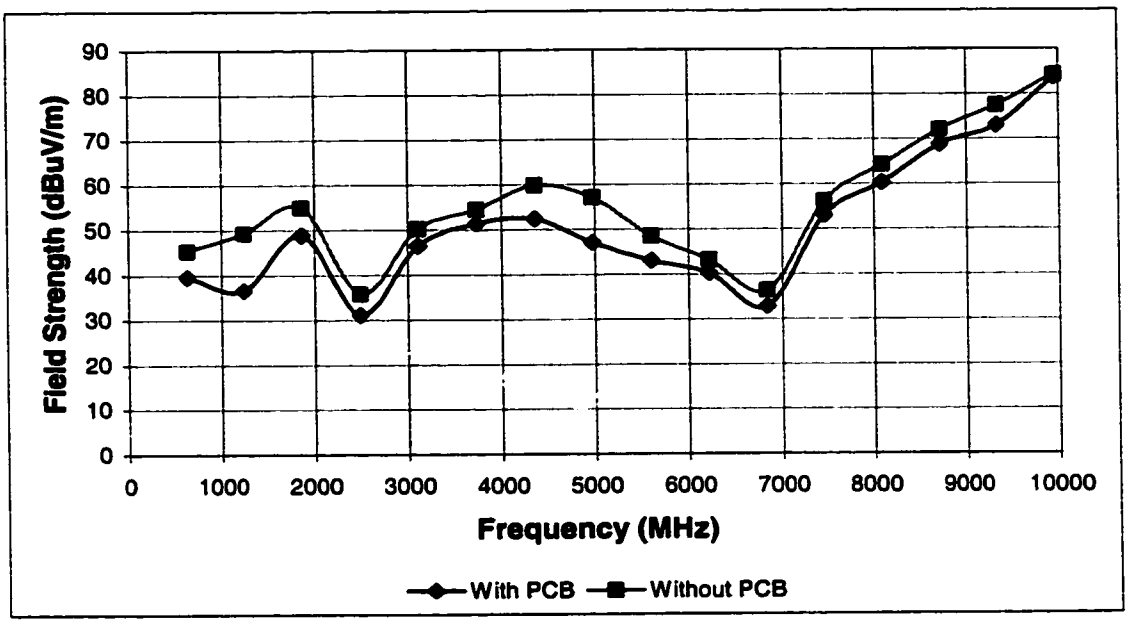

It is expected, from Figure 4-12, that shielding for the enclosure with PCB will be higher than the configuration without the PCB since field strength level coming from the test case with PCB is lower. It is not possible to point out with precision the resonance frequency from Figure 4-12 since it is a sample of discrete frequencies in a predetermined range. The following example illustrates the manner in which the Attenuation (SE) is calculated using values from Table 4-3. The rows in Table 4-3 and Table 4-4 are defined as follows:

Free Space Noise (dBμV) =	Peak voltage measured using the spectrum analyzer corresponding to the incident field strength for all polarization.
Max Free Space Noise (dBμV/m)=	Maximum peak voltage measured using the spectrum analyzer corresponding to the incident field strength for all polarization.
SE (dB) =	SE estimate. Amount of Attenuation provided by the enclosure at a specific frequency.

The value in the "Max free space noise" column is calculated by taking the maximum value of all possible polarization as the "Maximum free space noise". For the "Max enclosure noise" the column is calculated by taking the maximum value of all possible polarization as the "Maximum enclosure noise"; Equation 4-1 then defines SE, which is determined as follows:

Max Free Space Noise (dB μ V/m) – Max Enclosure Noise (dB μ V/m) = SE (dB μ V/m)

For example, in the at 622.08 MHz, Max free space noise is 95.82 dB μ V/m and the Max enclosure noise is 39.66 dB μ V/m then SE is calculated as follows:

95.82 dB μ V/m –39.66 dB μ V/m = 56.16 dB μ V/m or *56.16 dB* of Attenuation

Results have been plotted in the following figure for both configurations.

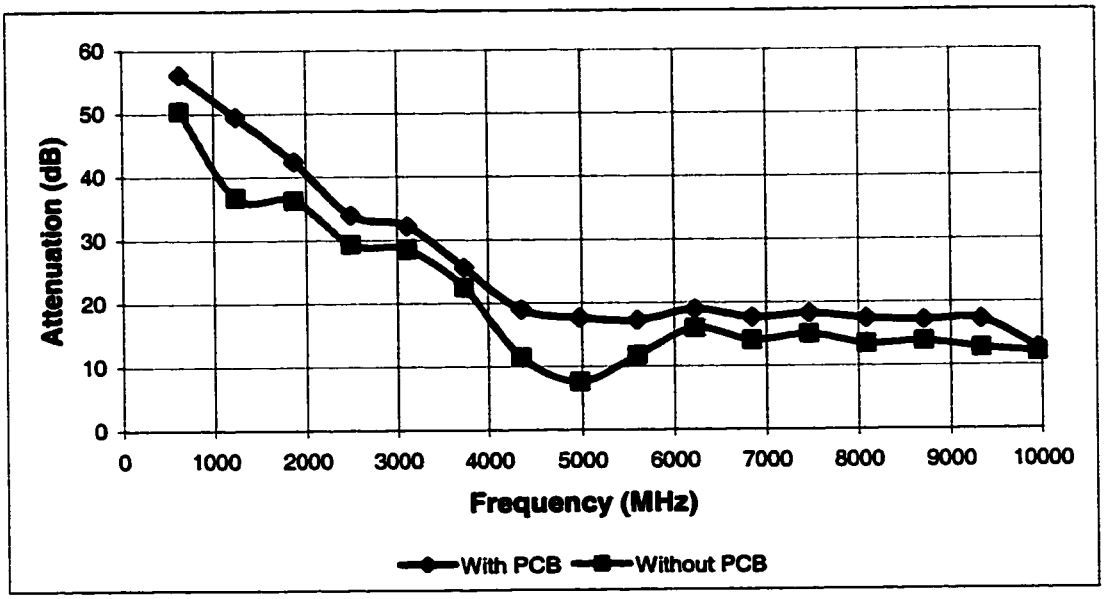

Figure 4-13: SE of the enclosure under test; test case with PCB and without PCB

4.5 Experimental Results Analysis.

Figure 4-13 shows that the shielding effectiveness has a minimum at about 5000 MHz for both test cases. The amounts of attenuation given by our two test cases are very low: between 4000 and 10000 MHz. The effects of the presence of the PCB only gives +/- 4dB of attenuation. The estimate in Chapter 3 indicated a similar increase (6.9 dB) for an enclosure with and without the PC B. The curve pattern of Figure 4-13 follows similar pattern as for the empirical analysis. Table 4-6 and Figure 4-14 show the variation of Q for the enclosure with and without PCB using Equation (3-17).

Table 4-6: Experimental values of Q for Aluminum enclosure with and without PCB.

Frequency (MHz)	Q with PCB	Q without PCB
622.08	80581.01388	64950.75621
1244.08	18949.48527	10458.97298
1866.08	5764.213911	4218.306197
2488.08	3728.405976	2780.293964
3110.08	2026.138892	1580.580624
3732.08	1883.384335	1449.384387
4354.08	4603.592161	1668.407087
4976.08	6963.539411	1291.64484
5598.08	2052.764641	947.642626
6220.08	807.2477784	573.4754116
6842.08	780.7754315	496.8611257
7464.08	526.8805344	357.891922
8086.08	516.1902721	306.9117948
8708.08	390.8752905	254.7104613
9330.08	374.548296	204.453278
9952.08	343.8617321	312.0405615

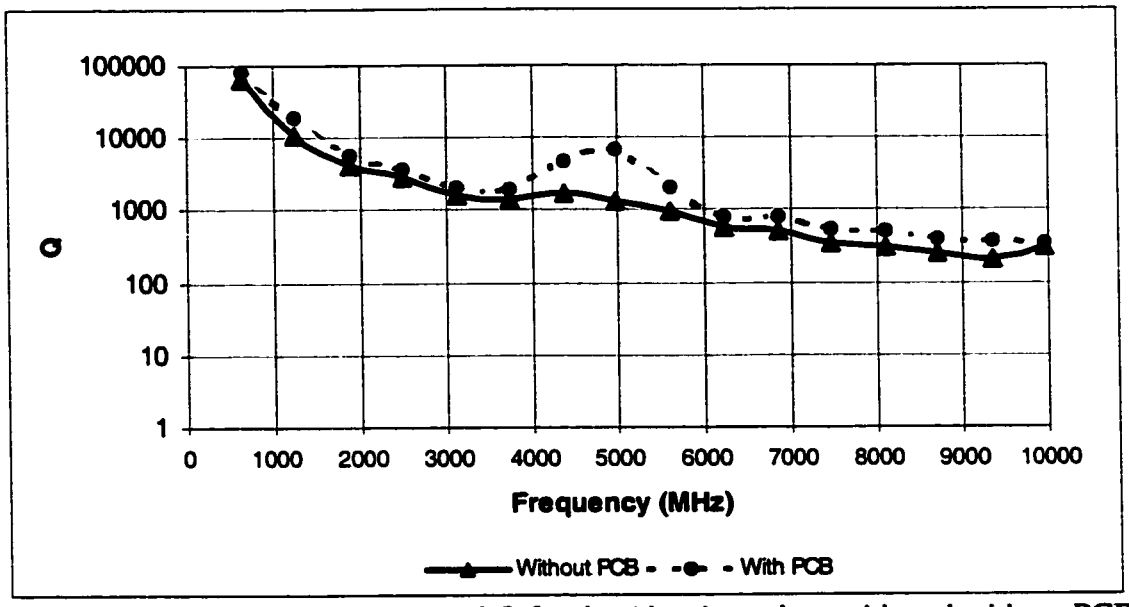

Figure 4-14: Value of experimental Q for the Aluminum box with and without PCB.

Figure 4-14 shows a large Q, at about 5000 MHz. Field strength at 5000 MHz inside the box is also large, and so we see a minimum in SE in Figure 4-13. The PCB presence reduces the Q at 5000 so the minimum in Figure 4-14 is not as deep.

EMC engineers can compare the SE target with the results obtained by this estimation method and conclude, generally, that more shielding is needed in the range: 4-6 GHz. Then, an attempt can be made to optimize the design with multiple hole patterns or different gaskets around the seams of the cover. For example, thermal engineers may want to do the experiment with an array of small holes instead of one big hole.

The inconvenience of experimental measurements is that every modification has to be done physically on the enclosure, restraining the amount and type of possible modifications. Time for testing and cost are also big issues in this case. However,

engineers consider this method more accurate and rely on its results to modify or validate their designs.

4.6 SE Experimental Estimation Discussion.

This kind of testing is impossible to do early in the design process. Mechanical engineers have to choose among a lot of variables and make many assumptions before arriving to the prototype unit. However, experimental measurements are the only way to verify the mechanical integrity of a shield. It is the only way to find mismatch materials, holes, and any mechanical malfunctions that can effect shielding. Time spent on shielding estimations in a laboratory is also expensive, and it should be noted that a single case study takes approximately one day to perform.

Nevertheless, experimental testing is recommended in conjunction with empirical studies. If both are correlating, the probability of passing the EMC requirement is higher. Other measurement methods can be used to estimate SE of small enclosures. The method presented here is simple and can give a lot of information on the emission source (angle, intensity) while doing the experiment. Engineers also use reverberation chambers to do shielding measurements by measuring the power coming out of the box. This method is also accurate for SE estimations but no information on the leakage point can be determined.

Further study of SE measurement methods is needed. Source and measurement equipment introduce too many uncertainties, and repeatability is also difficult using any

method. Changes in the noise source impedance in the shield and outside the shield have been neglected and, can be a source of errors in the technique. However, it is believed that at the frequency range of measurements (above 600 MHz) and small size of the radiator; 3 cm, make this assumption acceptable. The noise source may also be studied and better designed in order to match the antenna and frequency availability better.

Noise source impedance measurement, using a network analyzer, has been studied and practiced a lot in the high tech industry. [2][9] However, the availability of a network analyzer is crucial and far field estimations are done by empirical manipulations introducing certain risks of uncertainty.

All methods have a good and a bad side. At this stage, in SE measurements, no method has been determined to be the ultimate one. Engineers need to choose the estimation method by means of available equipments and sizes of EUT.

Experimental methods are well suited to validate a second type of SE estimation method, which are numerical simulations. The correlations between the two methods are always a good base too build confidence in such a tool.

CHAPTER 5

SE NUMERICAL SIMULATION

Numerical simulation tools have been used widely in the past 10 years [11][12]. They have improved significantly with the development of faster computer chips with larger memory. Most of the codes available today offer nice, friendly interfaces that reduces the burden of model definition. Design simulation is now possible with less time and can answer design questions at any step in a design process. [19]

In this study, Transmission Line Matrix (TLM) and Finite Difference Time Domain (FDTD) codes are used to determine the SE of our enclosure. A design approach is used to model the enclosure, such as simplification and time spent on modeling, which may be adequate for commercial practices. It would be a huge boom to EMC engineers if TLM or FDTD simulations were accurate enough for shielding design.

Excitation, for our model, is a plane wave, which follows the SE definition. Plane waves are easier to simulate than inside noise sources, due to unknown parameters: the noise source impedance and the voltage.

5.1 Transmission Line Matrix

Transmission Line Matrix (TLM) is a numerical code, invented in the late 70's that received, recently, a lot of attention and modification. TLM basics come from the work of Johns [21][35], which was later developed and made practical by Hoefer in 1985.

TLM employs circuit models of electromagnetic field problems defined as a network of discrete transmission lines connected at scattering junctions, in order to simulate the behavior of distributed system. The first TLM formulation, known as the "expanded node" formulation, was derived from lumped (RLC) model of transmission line equations, and later the most significant development has been the formulations for which the various field components were computed together at larger nodes instead of stagger. The "symmetric condensed node" such as the "hybrid symmetrical condensed node" is the result of further development of TLM. [13][40]

5.1.1 TLM Modeling

Modeling with our TLM code was facilitated by Computer Aided Design software (CAD). The enclosure model was simplified as much as possible, in order to show all-important details of the enclosure and reduce the amount of time spent for modeling. The radiation patterns obtained as a supplementary analysis (Section 5.5), suggest that the excitation should be a plane wave with $\theta = 90^0, \phi = 90^0$ degrees incident to the box; to achieve the "worst case scenario" of the four configurations, in Chapter 4.

The simple rectangular box, with dimensions given in Appendix B, had been model. Figure 5-1 shows three-dimensional view of the mesh configuration, the plane wave polarization (white cone) and the probes relative positions, in and out, of the enclosure.

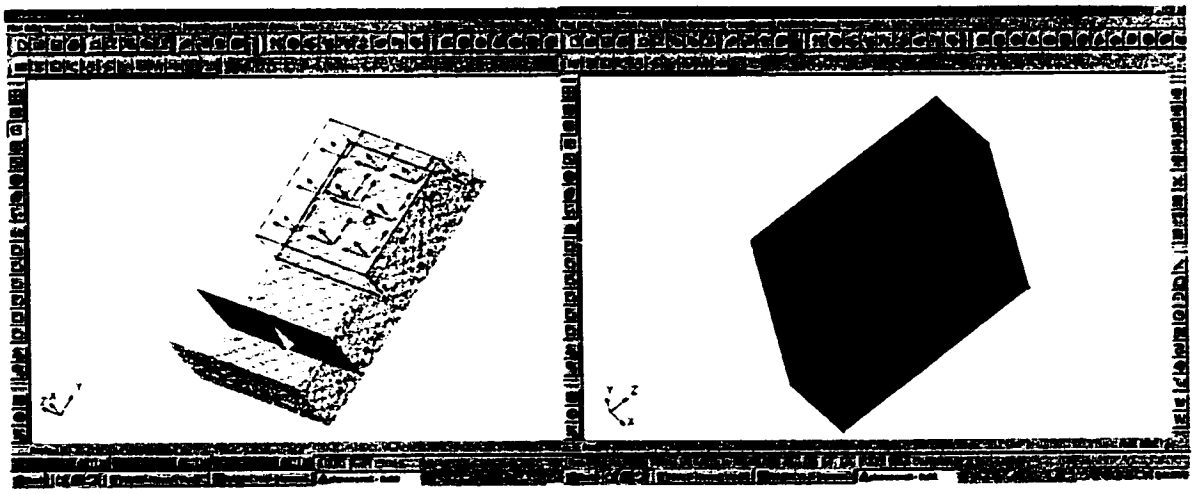

Figure 5-1: Model of the Aluminum enclosure without PCB.

5.1.2 TLM Result Analysis

The frequency responses of the two test cases to the 1V/m plane wave are presented in Figure 5-3 and Figure 5-4. The total field strength has been evaluated in the middle of the box in *mV/m*. The total field strength is the module of all E-field polarizations.

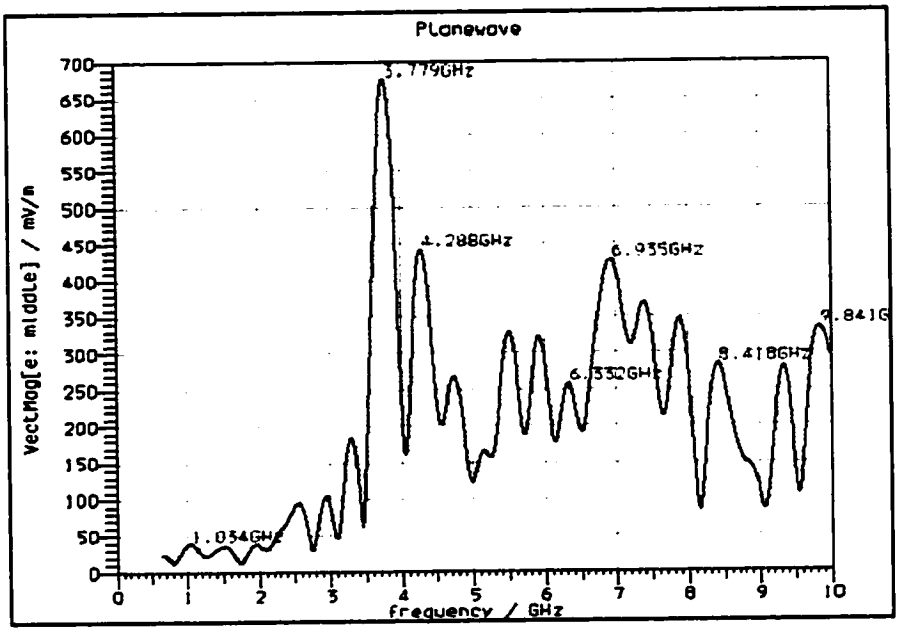

Figure 5-3: Frequency response of the enclosure without PCB.

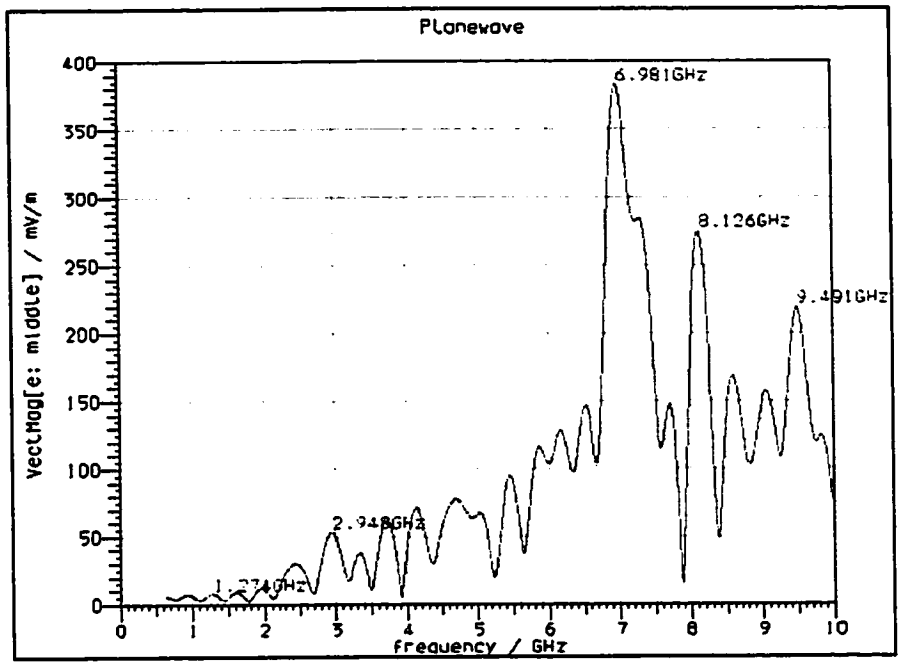

Figure 5-4: Frequency response of the enclosure with PCB

The TLM frequency response of our models, Figure 5-3 and Figure 5-4, shows several resonant peaks frequencies, eg: 1.034 GHz, 3.779 GHz, 4.288 GHz and 6.935 GHz for test case with PCB and 2.94 GHz, 6.981 GHz and 8.126 GHz for test case without PCB. It was calculated, earlier in Chapter 3, that the fundamental resonance (TE_{101} mode) was around 1.159 GHz. In our model, it appears at 1.034 GHz. The test case without a PCB shows less strong fields due to the presence of the PCB (lower Q).

Figure 5-5 presents the SE of the enclosure for both test case using normalization of Figure 5-3 and Figure 5-4 with Equation 4-1 the incident field is a plane wave of 1 V/m.

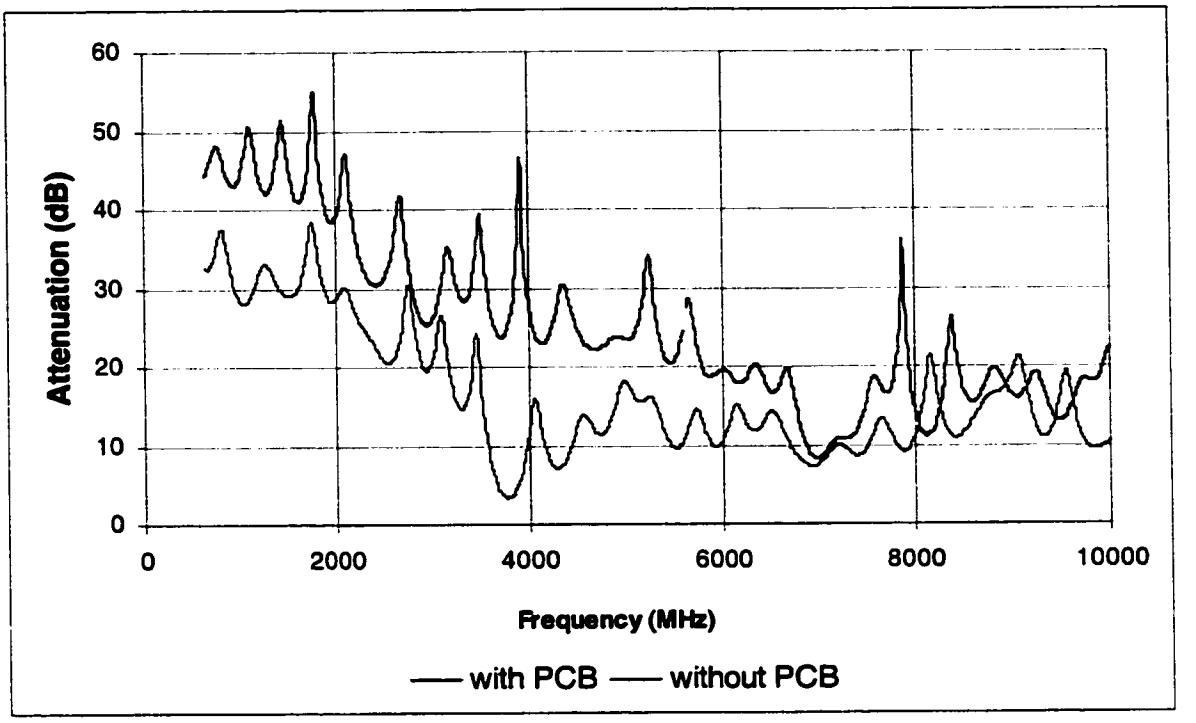

Figure 5-5: SE TLM estimate

The important data here is the lowest number. The lower the number, the worse the shielding of the box at that frequency. For example, at 3.878 GHz, The SE in Figure 5-5 is equal to 3.72 dB, which means that the enclosure provides the lowest attenuation (practically no shielding) at that frequency. The average difference between the Aluminum box with PCB and without PCB is 21.21 dB, which is around 3 times the 6.9 dB value from our empirical analysis. However, it was expected that the Q of the enclosure would introduce such separation.

SE results obtained from the TLM analysis are higher than the experimental and empirical analysis result. This can be due to the position of the probe. In our analysis, a

center point near the position of the experimental noise source was chosen arbitrarily and seems to be the worst case from the E-field strength distribution inside the box from Figure 5-6, 5-7.

One of the biggest advantages of numerical simulation is that the E-field distribution can be visualized. Figure 5-6 and Figure 5-7 show the E-field distribution over the inside cavities of the enclosure. Knowing the position of the weak and strong fields can be an asset for positioning the connectors, the cables and the ASICs. For instance, an engineer, with Figure 5-6, will be guided in a more confident fashion to position very important ASICs at the top left of the enclosure to eliminate possible emission problems. For emission reduction it is also clear that the test case study with PCB shows less field strength in general, as for test case without PCB.

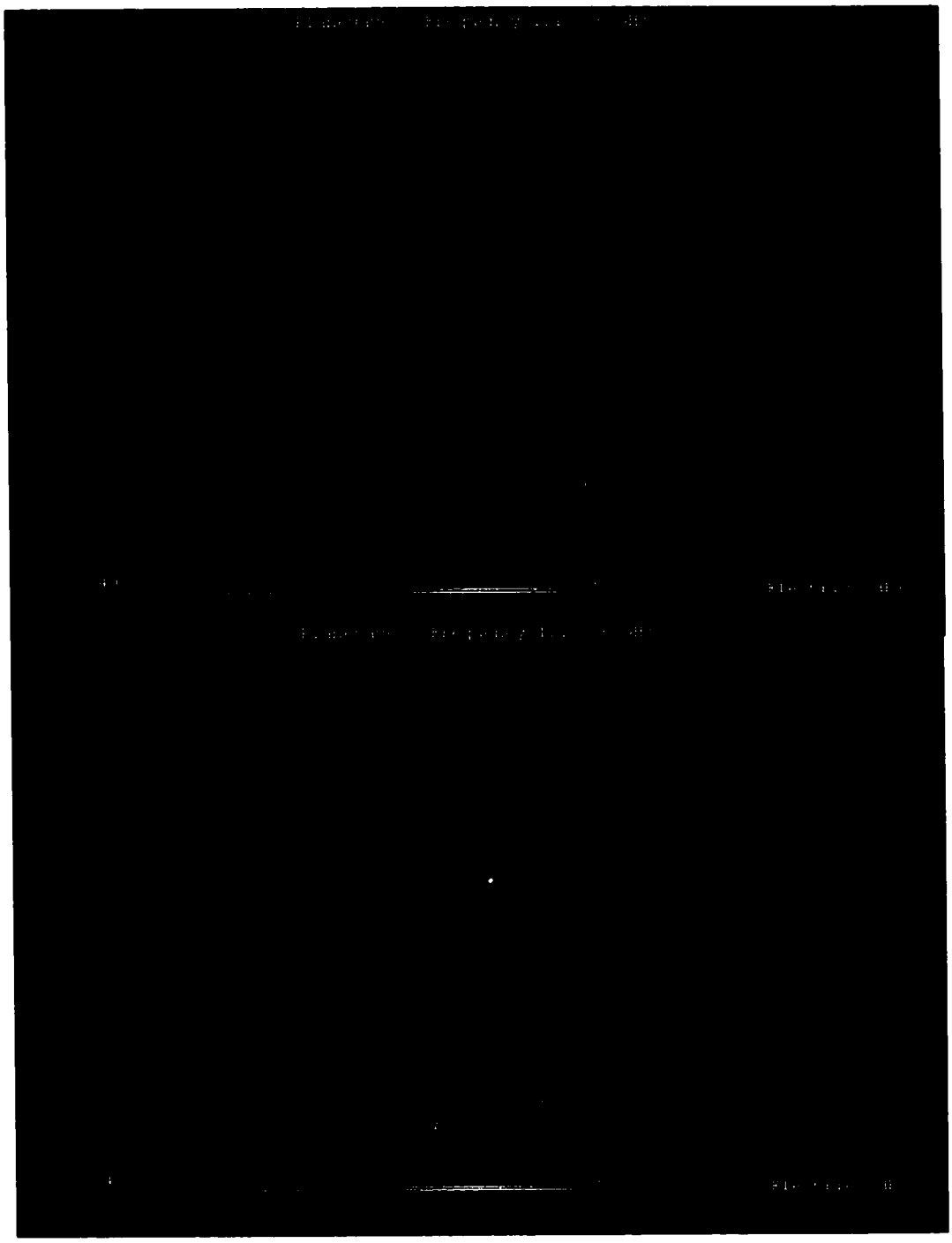

Figure 5-6: E-Field distribution without PCB.

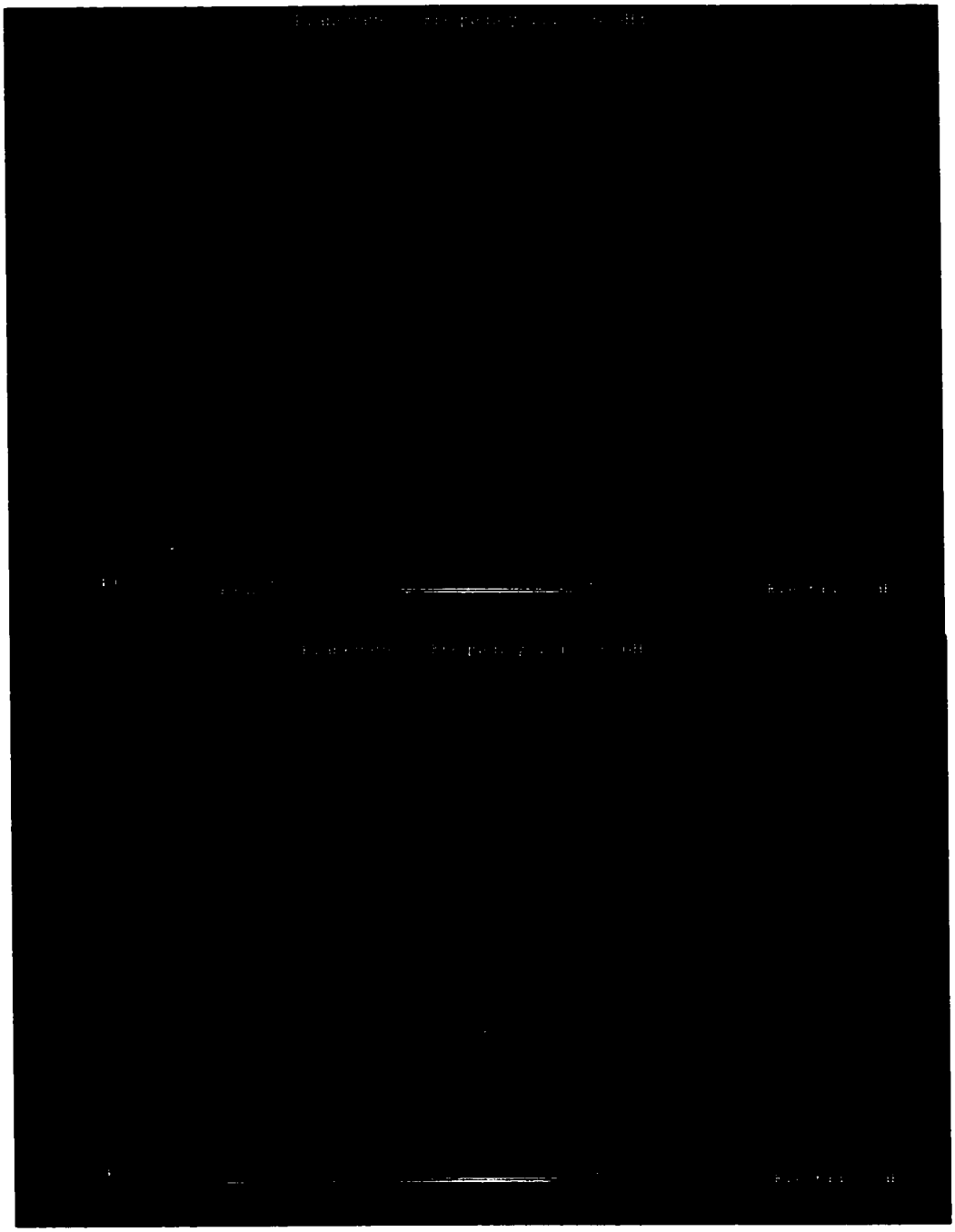

Figure 5-7: E-Field distribution with PCB.

5.1.3 TLM Supplemental Analysis

The TLM code can also predicts the far-field emission, which can be compared to the standard limits. This kind of result can be very useful while optimizing an enclosure design. However, experimental baseline and TLM baseline results must be used to help evaluate the real quantitative value obtained by the simulation.

To perform a better comparison with the empirical and experimental result presented in this thesis, the approach of a small dipole radiating inside the enclosure, is partially studied.

In order to accomplish such a radiated emission estimate, our model needs to be modified. The major modification is the excitation of the model; in this case a small wire, driven by a voltage of 0.01 V is used. Figure 5-8 shows the modified model with its excitation. A PCB board has been placed inside the enclosure with a small wire, covered with a square heat sink plate of 2 cm side and 2 mm thickness, representing the VCO. The battery is represented by a 4 cm by 2 cm by 2 cm lead (Pb) block.

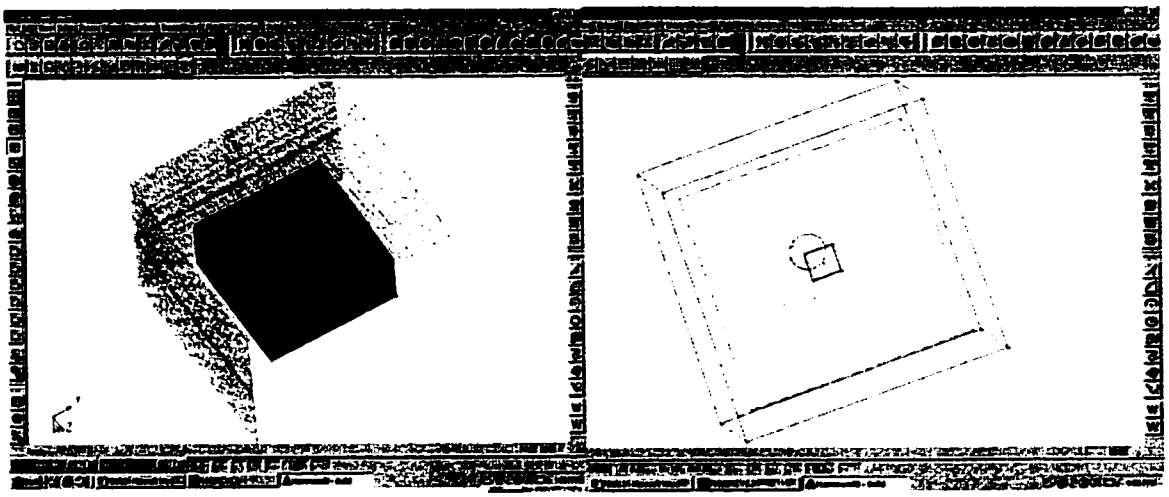

Figure 5-8: Model of the enclosure with internal noise source.

5.1.3.1 TLM Supplemental Results Analysis

The frequency response of the model with the internal noise source is presented in Figure 5-9. The curve shows similar peaks resonant as the plane wave simulation.

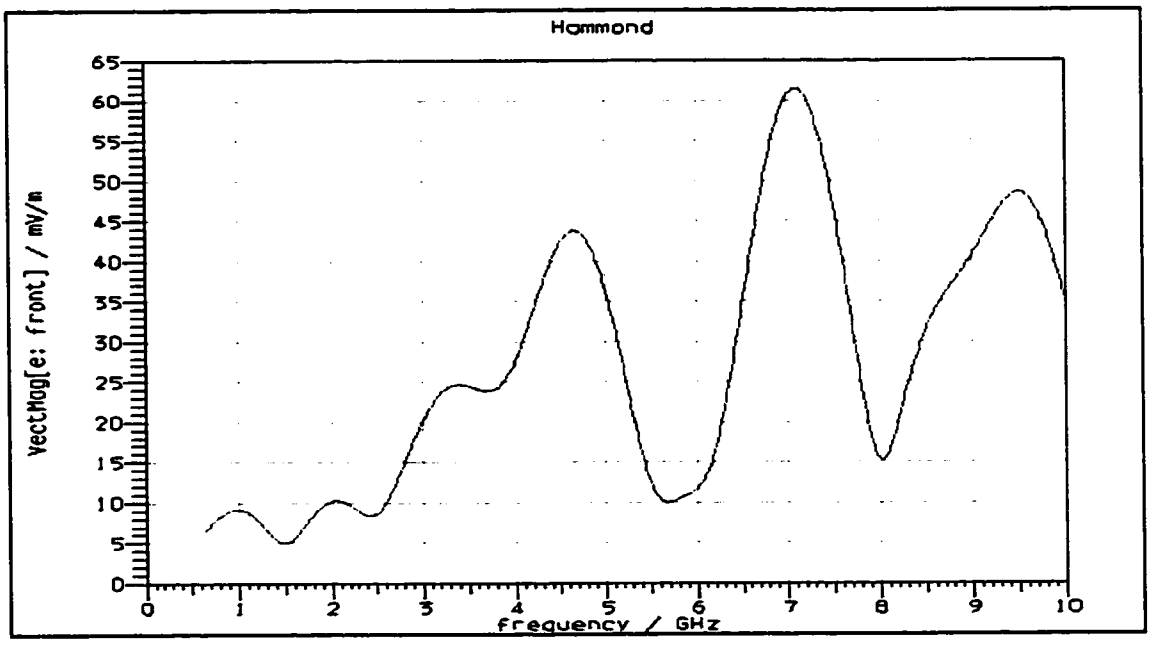

Figure 5-9: Radiated Field at 3m.

Results obtained are projected at a distance of 3 m., which is considered in the plane wave region of our box and can be compared to the standard limit of Table 2-1 and Figure 2-2. For example at 622.08 MHz the peak measurement is 6 mV/m., which equals |75.56| dBuV/m. (|20log (6000 uV/m.)|). The limit for FCC Class A at 622.08 MHz is 56.4 dBuV/m., which makes our enclosure non compliant by 19.16 dB uV/m. However, such comparison should only be made when experimental results are available to correlate the model results.

A SE estimate using an internal source can, probably, be done if the inside source is well known (impedance). However, this subject will not be presented in this thesis but would be included in further research on the subject.

The radiation pattern of the Aluminum enclosure is also a parameter of great interest. It indicates the behavior of the enclosure spatially, as a radiator. By knowing the radiation pattern, the engineer can adjust the design, to reduce the emission lobe by using frequency selective materials [3]. The radiation pattern of our model at 622.08 MHz is shown in Figure 5-10. The figure shows the 'total field" as a function of direction, and that the "total field" is $\sqrt{E_x^2 + E_y^2 + E_z^2}$.

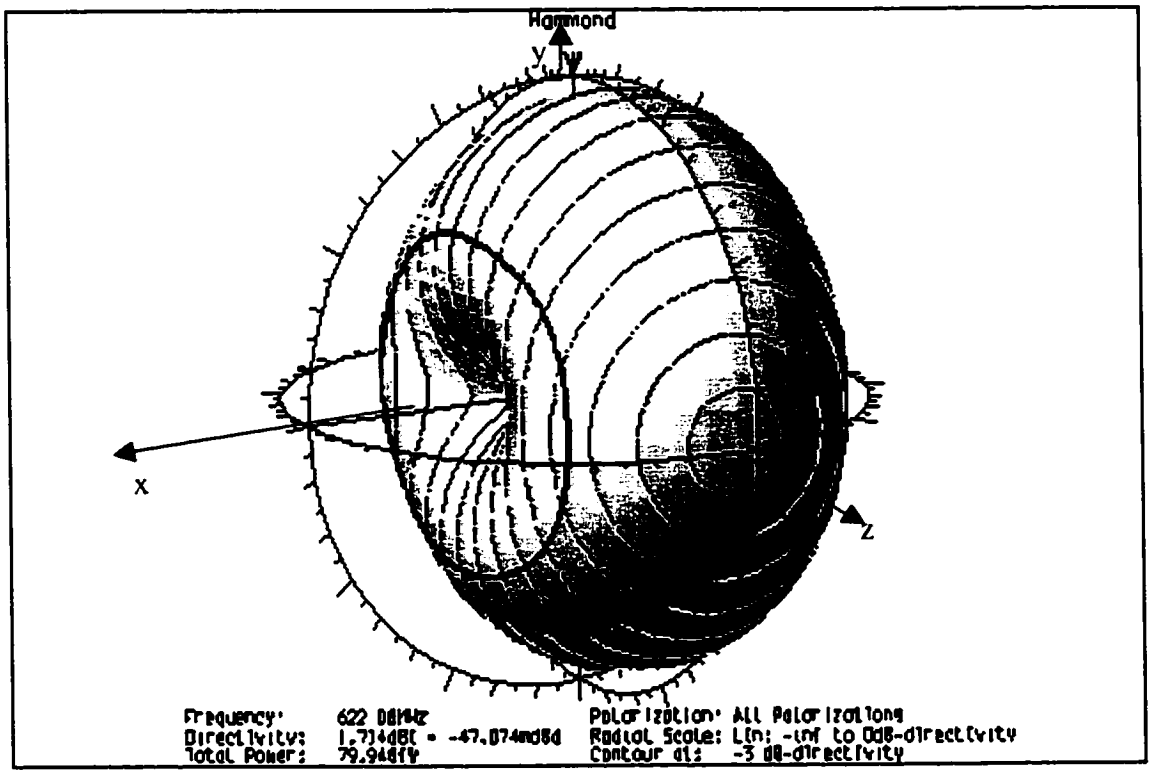

Figure 5-10: Radiation pattern in 3-D of the Aluminum enclosure with internal source

The doughnut shape of the radiation pattern is the direct result of the hole reacting as a small loop antenna in the plane of the hole. This shape is also identical to a small dipole perpendicular to the hole, oriented parallel to the x-axis. The choice for the plane wave incident polarization and orientation of Section 5.1.1 and 5.2.1 can be supported using Figure 5-10. The maximum emission point is oriented in the *y*-axis direction and gives suggestion for $\phi = 90$ degree.

5.2 Finite Difference Time Domain

FDTD codes have been used a lot for academic purposes. Mechanical and chemical engineers used this numerical method to predict structure and exchange reactions. In electromagnetics, FDTD have been used to solve shielding, emission behavior and antenna problems. Developed by Yee [34] in the mid 1960, this numerical code has seen an explosion of development and application. The main idea behind the code is the direct application of the Maxwell's differential equations. [11][12][13] The code used in this thesis is an FDTD academic version. Capabilities of the software are limited but easily expandable to match a commercial code.

5.2.1 FDTD Modeling

Following the same structure as for the TLM model, the enclosure was modeled as a simple hollow box. A file editor was used to describe the geometry, as in Appendix G. The lowest frequency of interest is 600 MHz. Only one material is defined, material #1, which is "perfect electric conductor" or "PEC" by convention. This material is used to define the enclosure wall and PCB. The excitation is an incoming plane wave from direction $\theta = 90^0, \phi = 90^0$, following the positive +y axis. The amplitude is 1 V/m oriented in the +*x* direction. The box is modeled and oriented with the cover having the hole in the *xy*- plane. The hole is centered on the origin. Figure 5-11 below, presents two views of our model.

Figure 5-12, show the enclosure views with a 2 mm thick PCB.

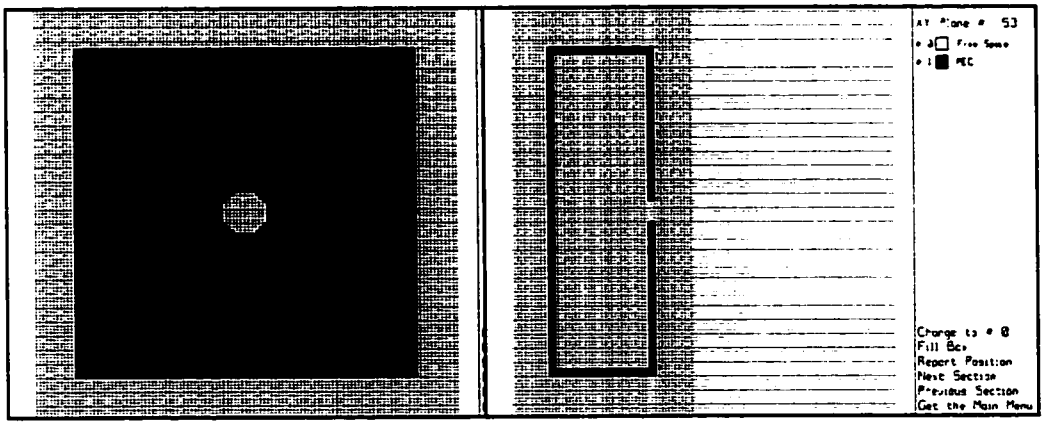

Figure 5-11: FDTD model cross-section view without a PCB (showing cover)

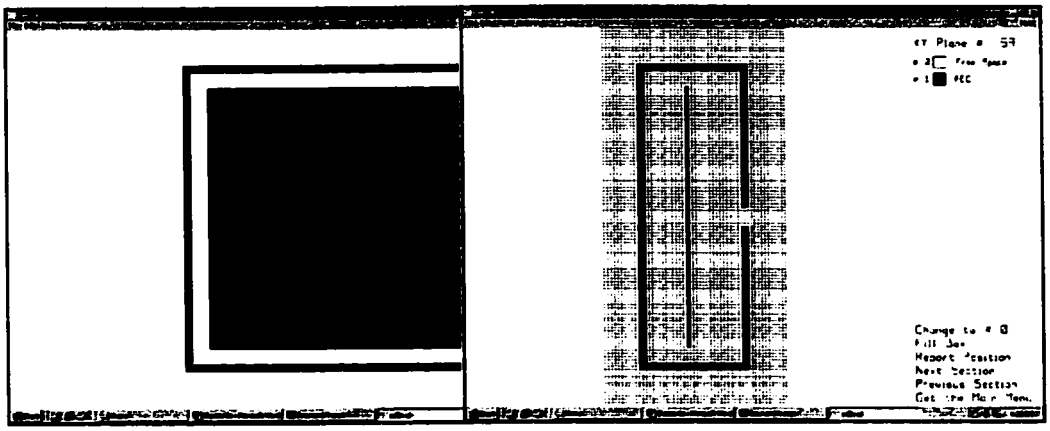

Figure 5-12: FDTD model cross-section view with a PCB.

5.2.2 FDTD Result Analysis

It is possible with the FDTD code to view the field distribution in the box for different planes. Figure 5-13 and 5-14, presents a typical cross-section view of our enclosure without and with PCB.

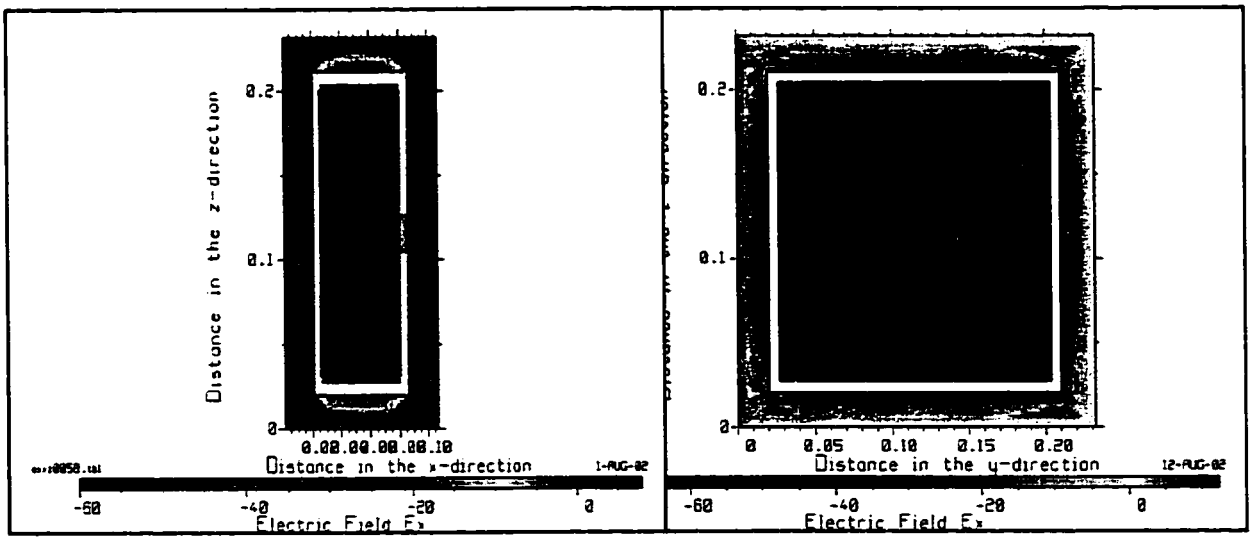

Figure 5-13: Cross view of E-field distribution without PCB

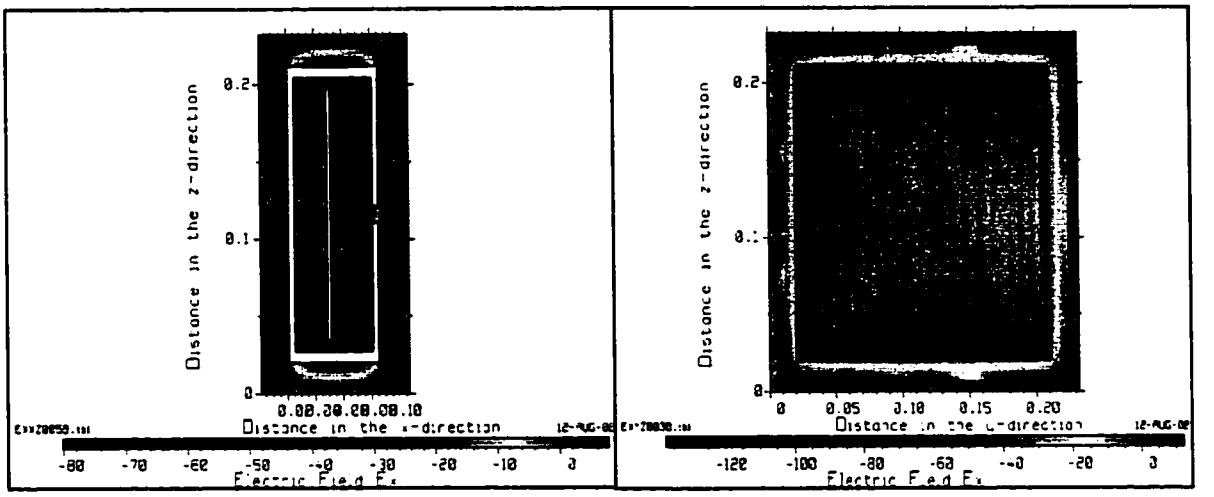

Figure 5-14: Cross view of E-field distribution with PCB

The walls of the box are made of PEC or Perfectly Conducting Material and from this, it is expected that the fields inside the walls to be exactly equal to zero. However, the cancellation of the "incident" plane wave field and the "scattered" field in the walls is imperfect, so the field inside the walls is about 90 dB down from the incident plane wave, which can be consider to be 0 dB. The color scale in Fig. 5-13 and 5-14, is such that fields lower than -65 dB is graphed in white; hence, most of the volume of the walls are shown in white. The field inside the box is remarkably constant for both test, especially with PCB from figure 5-13, 5-14. The field strength varies somewhat with position but overall it is 30 dB down from the value of the incident plane wave.

One-way to define "Shielding Effectiveness" is to take the value of the field at a typical point inside the box; then (E_z /E_{inc}) is the Shielding Effectiveness. It might be more meaningful to use the average value of the field over the interior volume of the box. Or, perhaps, the field over an important region could be averaged. However this will have taken additional time and process.

SE estimation using FDTD is presented in Figure 5-15 for both test cases. Emission levels were taken manually from the software in the middle of the enclosure , at coordinate (-2.775,0,0), to compute the SE with equation 4-1. Table 5-1 presents cumulated values use for SE FDTD calculation. From Figure 5-15, the enclosure with PCB shows more shielding due to its lower Q value. Maximum shielding is obtained at 622.08 MHz and the minimum is located at 10 GHz, 10 dB. Shielding starts to be constant after 4 GHz up to 7 GHz. The difference between the 2 curves, with and without PCB is around 2.71 dB, which is half the empirical value and a lot less then the TLM simulation. Model simplification can be a factor influencing those results.

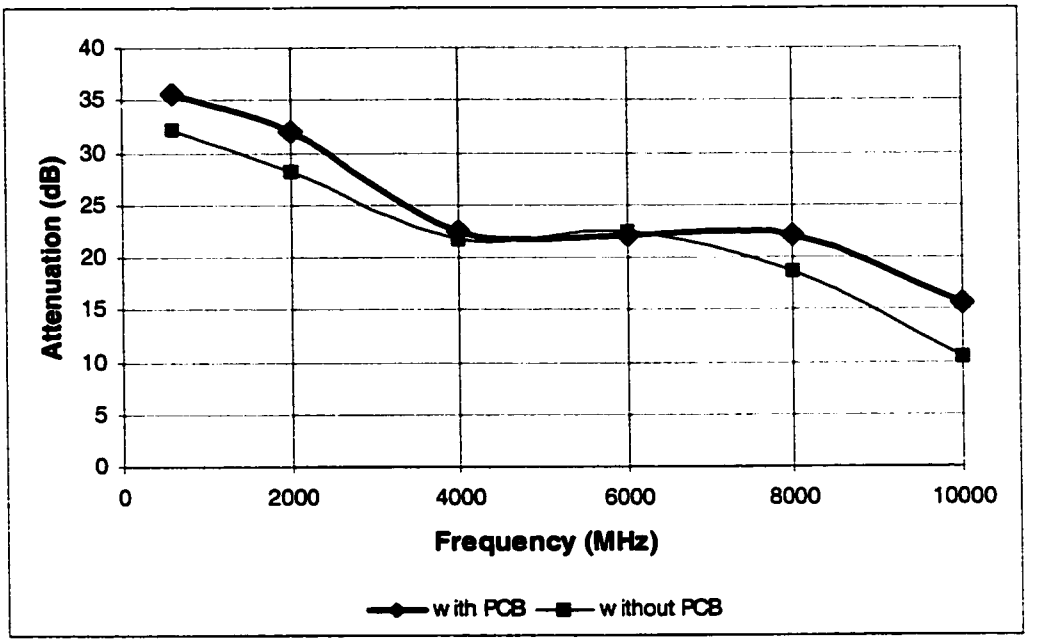

Figure 5-15: SE estimate using FDTD

Table 5-1: FDTD simulation results.

Frequency (MHz)	Without PCB		With PCB	
	Field Strength (dB V/m)	SE (dB)	Field Strength (dB V/m)	SE (dB)
600	-32.28	32.28	-35.62	35.62
2000	-28.22	28.22	-32	32
4000	-21.66	21.66	-22.45	22.45
6000	-22.46	22.46	-22.17	22.17
8000	-18.58	18.58	-22.07	22.07
10000	-10.5	10.5	-15.68	15.68

5.4 Numerical Simulation Discussion

Numerical simulations are great design tools, since they can be used at any stage in a design process. Model can be made with little information and updated on the way with ease. However, results obtained are only good as what you model.

In the past two years, numerical simulations have attracted a lot of interest in the design industry. The cost of using simulation tools is less expensive than using a 3m chamber or any lab accessories. Simulation can be done at different levels; PCB, module and shelf level. Time spent on modeling and run time is the only disadvantage that can become advantage if model is used repeatedly. Numerical tools and model used by Chemical and Mechanical engineers are often compatible and can be employed to save modeling time. Some commercial codes also offer converter tools to import model from CAD tools, like ProE and AutoCAD.

Using a numerical tool efficiently in a design process, necessitate a lot of practical experience. More measurements and simulation results of real designs are needed in order to build confidence in design capability of the software.

In this thesis the modeling took an average of 20 minutes for the TLM and FDTD code. Modeling can be much longer depending on the complexity of the model.

Computing time for TLM was 45 minutes for one test case study, and for FDTD 14 hours, for one test case study. Time is an important cost aspect in design and should

be kept as low as possible. FDTD requires the entire volume to be mesh compared to TLM, where the mesh can be adjusted to the part of interest in the model. This is the main reason of the long computational time.

Comparison of results between TLM and FDTD are presented in Figure 5-16. TLM show more separation between the two test case studies then any methods (21.21 dB). From 622 MHz to 2.5 GHz. The FDTD values are lower by 10 dB, for the case with PCB and are a perfect match, for the case without PCB. Between 4 GHz to 8 GHz, TLM values are very unstable. FDTD are more uniformed for both test cases.

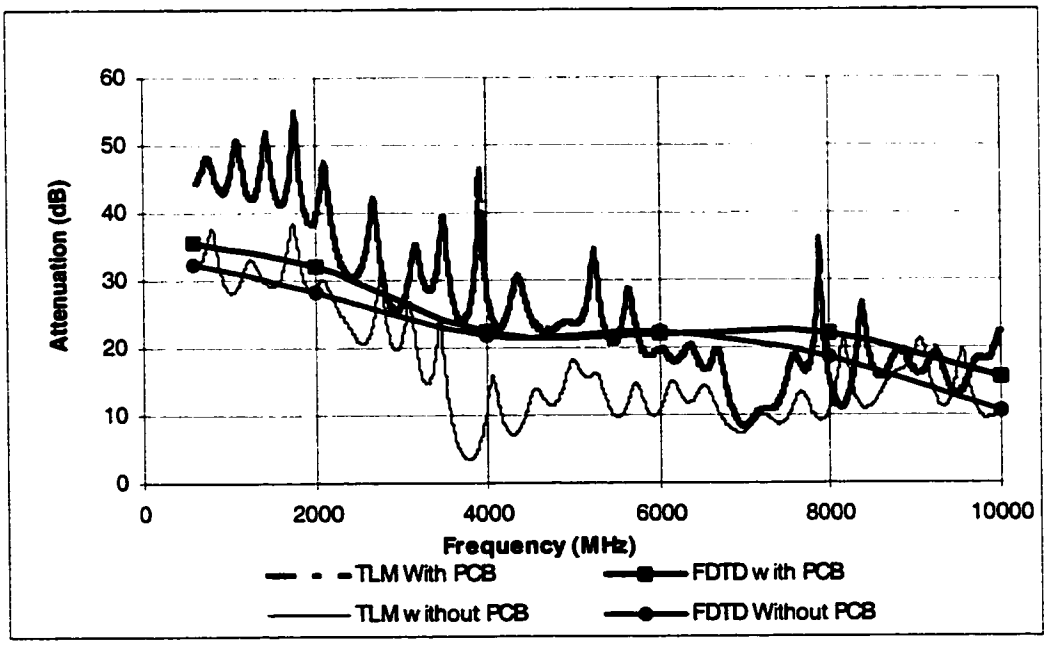

Figure 5-16: SE comparison between TLM and FDTD

FDTD and TLM are two numerical methods used in electromagnetics. Other numerical codes can be used to determine SE:

1. Moment Method (MoM),
2. Finite Element (FEM),

Free codes can also be found on the Internet. The most popular is NEC [13].

With computer and programming evolution, numerical codes are going to improve with time. Engineers have only started to feel the basic uses of those codes. Many are still skeptical and they rely on experimental measurement for design purposes. Experience, in both experimental and numerical simulations, needs to be done to establish modeling guidelines and quantitative result interpretations.

Further study needs to be done on modeling of the excitation source. Accurate prediction of far-field emissions from this kind of source can be very useful for pre-compliance studies.

CHAPTER 6

SE ESTIMATION METHODS COMPARISON

The three SE estimation methods used in this thesis were not developed to be compared directly with each other. However, the intention of this study is to compare the information obtained plus the usefulness of each method in the EMC design process. The direct comparison of the results will be made with caution, whenever possible.

SE estimation is a very controversial subject. No real methods have been adopted by the design industry. The scientific community uses the definition and measurement protocol defined by MIL-STD, which give optimistic results of SE.

6.1 Method Comparison for Design

The empirical method is the first method to be used in a design process, since it is the simpler and easier to apply. At the architectural level of the project, question arises on the sizes of holes allowed and approximation values of SE. This method is perfectly suited to answer such questions. The empirical analysis needs only basic enclosure dimensions to evaluate SE. Time needed to establish SE values is shorter then the experimental and simulation methods. On the negative side, this technique is completely ineffective for complex enclosures.

Experimental estimation is the most used in the industry. Experience has made this technique efficient and reliable. Results obtained are very close to the finished product, since we used a physical prototype, which included most of the geometry details. Time spent for SE evaluation and costs of laboratory time, are the main disadvantages of this method. SE results obtained are also limited to discrete frequency due to the ECL clock. A minimum of 1 day is expected for compiling experimental analysis.

Numerical simulations are the newest SE estimation techniques. Their application up to now, have only been made to the PCB traces (signal integrity) and simplify enclosure levels (vents and wave guides). Results obtained by simulations are mainly affected by how the model is defined and simplified. Correlation with experimental results needs a lot more work. The usefulness of the numerical simulation is the ability to see the field distribution. It can also verify changes without resulting in irreversible physical alterations of the prototype. Numerical simulation can be used anywhere in the design process, as long as basic dimensions and objects can be model. Using numerical simulation is time consuming. The preparation of the model takes most of the time. In some applications, the model is prepared automatically from CAD drawings of the device, and this speeds up the simulation time. The typical simulation analysis takes around 1 day. Time for simulation can be shortened if model is used repeatedly. The following figures indicated best use of each method in the design process.

6.2 Direct Method Comparison

To compare the estimation method, the results for each SE estimation of the Aluminum enclosure with PCB will be used. The more pessimistic result is the experimental estimation, which is understandable due to the sampling and factor neglected in measurement (noise source impedance change). The numerical simulation, TLM, results shows more information, resonance peaks, then any of the other two methods.

SE results from the three methods are compared in Figure 6-1; the empirical, experimental and simulation SE estimation results are closed and follow a similar curve pattern.

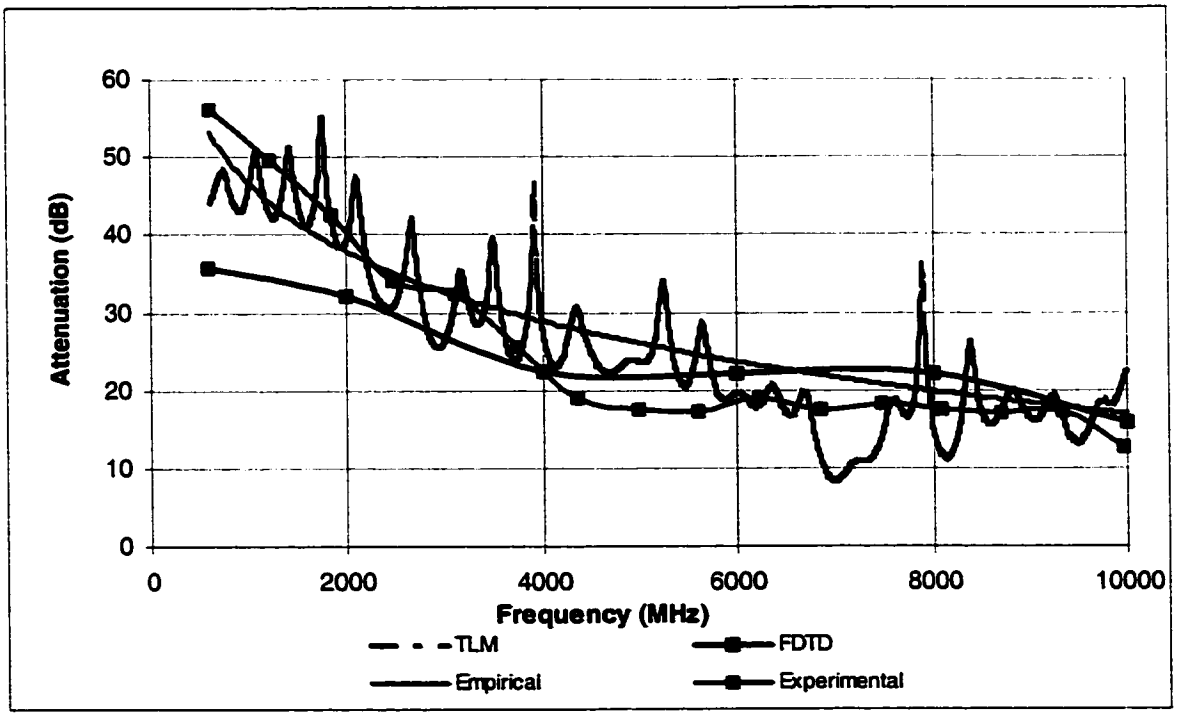

Figure 6-1: SE comparison curve: empirical, experimental and simulation estimates.

The Figure 6-1, shows that the empirical estimate, very nicely, predicts the "trend" of the SE computation with TLM, from the incoming plane wave. The measured and FDTD curves, mostly fall below the TLM and the empirical curves. The TLM curves has a minimum around 7 GHz, suggesting that something is missing from the TLM model that is important in this frequency range. Same remark for the FDTD result from 622.08 MHz to 4 GHz values are relatively lower then any estimation methods suggesting that our model may be too simplified

The best method cannot be pointed out. The use of each method is more related to its usefulness at the particular stage of the design process. During development, a designer uses a mix, of the three methods, to obtain better confidence that the enclosure SE is enough to pass the standard limits.

CHAPTER 7

CONCLUSION

7.1 Highlights

Three SE estimation methods have been presented:
empirical, experimental and numerical simulations.

The SE of an Aluminum enclosure, with an aperture in the middle of the top cover, was evaluated, using the three above mentioned methods. Two test cases of the enclosure, with and without PCB, were investigated. The PCB presence inside the cavity, lowered the value of Q, which in turn increased the SE of the box. The volume and radius of the hole were also parameters that influenced greatly the SE.

SE results are similar from each estimation method. However, EMC design information, obtained by each method, is different. Chapter 6 reinforced this statement, and gives the summary of all SE results. The simulation and experimental method offer the possibility to identify resonance frequencies and leakage positions, respectively. Their uses are also limited by the information available at the time of the design. At each step, in an EMC design process, an SE estimation found its place. In the beginning, when concept and architecture takes place, the empirical estimate is the most suited. After completion of a prototype model, the experimental estimate can be the best option to evaluate SE. Numerical simulation is a tool that can be used during the whole EMC

design process. However, results are clearly dependent on the model simplification and need to be correlated with experimental results in order to gain more confidence.

7.2 Contribution

The application of SE estimation methods for small enclosures was the contribution of this thesis. SE estimates have been compared with SE measurements using an industry-standard test method, and with numerical simulations of the SE, using TLM and FDTD. It was concluded, in Chapter 6, that both experimental and computational methods are good to approximate SE. For SE estimates, the numerical simulations give more information on the enclosure EM behavior, resonance peaks, regions of high field strength and radiated emission predictions. The thesis demonstrates that, the SE of an empty enclosure compare with the SE of an enclosure containing a printed circuit board (PCB), differs by 2.71 to 21 dB, due to the cavity loading. Numerical simulation seems to be the new way of designing. The designer is more at ease because of rapid change and ability to see the invisible.

7.3 Recommendation for Further Work

More studies need to be done in the area of the experimental estimation methods, in order to verify the impact of the noise source impedance changes with and without the shield. The simulation would be most useful if all the details of an enclosure, could be modeled: all holes, wires, all PCBs and so on. This is possible with FDTD or TLM and

would give a much more realistic assessment of the radiated emissions from a device. However, it is time consuming and noise source modeling needs to be studied in order to model them accurately.

The full spectrum of the SE could be obtained from FDTD in one run, using a Gaussian pulse source. The FDTD shows that the model may have been to simplified for this numerical code. A more detailed model would have to be investigated to achieve similar results as with the experimental method.

No protocol or directly proven methods have been established as the ultimate and perfect one. SE estimation is used to build confidence in the design of a shield in order to pass regulatory tests. Actually, the regulatory compliance testing is the goal of the SE estimate for which it is intended to achieve a pass with confidence.

REFERENCES

[1] L.T. Gnecco, "The design of shielded enclosures – cost-effective methods to prevent EMI," Newnes, Boston, 2000.

[2] Cromarty, "Effect of apertures and enclosure dimension on the shielding effectiveness of electronic product enclosures," Concordia University, Montreal, 2001.

[3] M.Li, S. Radu, Y. Ji, J. Nuebel, W. Cui, J. L. Drewniak, T. H. Hubbing, T.P. Vandoren, "EMI from apertures at enclosure cavity mode resonances," IEEE Electromagnetic Compatibility Symposium, Austin, TX, pp.183-187, Aug. 1997.

[4] M.P. Robinson, J.D. Turner, D.W.P. Thomas, J.F. Dawson, M.D. Ganley, A.C. Marvin, S.J. Porter, C. Christopoulous, "Shielding effectiveness of a rectangular aperture," Electronics Letters, Vol 32, Number 17, pp.1559-1560, August 1996.

[5] J. Rollin, G. Arcari, G. Wong, "Method of testing shielding effectiveness and electromagnetic field generator for use in testing shielding effectiveness," Nortel Networks, 1998.

[6] UL Software, "Amplitude," version 6.0, 2001

[7] H. Ott, "Noise reduction techniques for electromagnetic in electronic systems," 2nd Edition, Wiley-interscience, Toronto, 1988.

[8] MIL STD 285, "Military standard attenuations measurement for enclosures, electromagnetic shielding, for electronic test purposes, method of," United States government printing office, Washington, 1956.

[9] IEEE, "IEEE Standard for Measuring the Effectiveness of Electromagnetic Shielding Enclosure," IEEE Std 299-1991, IEEE, July 1991.

[10] N. A. McDonald, "Simple approximations for the longitudinal magnetic polarzabilities of some small apertures," IEEE Transaction Microwave, vol 36, pp.689-695, July 1988.

[11] Li, M., Ma, K.-P., Hockanson, D.M., Drewniak, J.L., Hubing, T.H., Van Doren, T.P., "FDTD modeling of thin-slots near corners of shielding enclosures," IEEE Transactions on Electromagnetic Compatibility, August 2000.

[12] Li, M., Radu, S., Nuebel J., D.M., Drewniak, J.L., Hubing, T.H., Van Doren, T.P., "Reducing EMI through shielding enclosures perforations employing lossy materials: FDTD modeling and experiments," Proc. of the 13th ACES Symposium, Monterey, California, March 17-21, 1997.

[13] UMR; www.umr.edu

[14] Bruce Archambault, Omar Ramahi, "Evaluating tools which predict the shielding effectiveness of metal enclosure using a set of proposed standard EMI modeling problems," International Symposium on Electromagnetic Compatibility, pp.517-521, August 1998.

[15] H. A. Bethe, "Theory of diffraction by small holes, Physical Review," vol. 66, pp. 163-182, 1944.

[16] Collin R. E., "Foundation of microwave engineering," Mc Graw-Hill Inc, New York, 1992.

[17] C.A. Balanis, "Advanced engineering electromagnetics," John Wiley & Sons, New York, 1989.

[18] Clayton Paul, "Introduction to electromagnetic compatibility," John Wiley & Sons, New York, 1980.

[19] Min Li, James. L. Drewniak, Member, IEEE, Sergiu Radu, Joe Nuebel, Todd H. Hubing, Senior Member, IEEE, Richard E. DuBroff, Senior Member, IEEE, and Thomas P. Van Doren, Senior Member, IEEE, "An EMI estimate for shielding enclosure evaluation," IEEE Transaction on electromagnetic Compatibility, Vol. 43, No. 3, August 2001.

[20] ANSI C63.4, "Methods of measurement of radio noise emission from low-voltage electrical and electronic equipment in the range of 9kHz to 40 GHz," American National Standards Institute, New York.

[21] TLM, Dr. David Johns, Flomerics Inc., Massachusetts, Boston, USA.

[22] Ma, K.P., Li, M., Drewniak, J.L., Hubing, T.H., Van Doren, T.P., "A comparison of FDTD algorithms for subcellular modeling slots in shielding enclosures," IEEE Transactions on Electromagnetic Compatibility. August 1964.

[23] Ko, W. L., Mittra, R., "A comparison of FDTD and Prony's methods for analyzing microwave integrated circuits," IEEE Trans. Microw. Theory Tech., vol. 39, pp. 2176-2181, December 1991.

[24] J. D. Krauss, "Electromagnetics," 4th Edition, McGraw-Hill, New York, 1991.

[25] J. D. Kraus, "Antennas," 2nd Edition, McGraw-Hill, New York, 1988.

[26] H. Y. Chen , I-Y. Tarn, and Y-J. He, "NEMP fields inside a metallic enclosure with an aperture in one wall," IEEE Transaction Electromagnetic Compatibility, volume 37, pp.99-105, February 1995

[27] J.J. Rollin and G. Arcari, L. Roy, "A novel technique for measuring IC package shielding effectiveness," 16 Th IEEE IMTC/99, May 24-26, Venice Italy 1999.

[28] Ramo, S., Whinnery, J. R., Van Duzer, T., "Fields and waves in communications electronics, John Wiley & Sons, Inc., New York, 1994.

[29] Collin, R. E., "Field theory of guided waves," IEEE Press, New York, 1991.

[30] Marcuvitz, N., "Wave guides handbook,' Peter Peregrinus Ltd., London, 1986.

[31] Butler, C. M., "A formulation of the finite length narrow slot or strip equation," IEEE Transactions on Antennas and Propagation, vol. AP-30, pp. 1254-1257, November 1982.

[32] Sarkar, T. K., Pereira, O., "Using the matrix pencil method to estimate the parameters of a sum of complex exponentials," IEEE Antennas and Propagation Magazine, vol. 37, No. 1, pp. 48-55, February 1995.

[33] Gilbert, J, Holland R., "Implementation of thin-slot formalism in the finite-difference EMP code THREDII," IEEE Transactions on Nuclear Science, vol. NS-28, pp.4269-4274, December 1981.

[34] Taove, A., "Computational electrodynamics- the finite-difference-time-domain method," Artech House, Inc., Norwood, MA, 1995.

[35] Robert E. Collins, "Field theory of guided waves," IEEE Press, 2nd Edition, Piscataway, NJ.pp288-289, 1991.

[36] Horacio A. Mendez, "Shielding theory of enclosure with apertures," IEEE Transactions on Electromagnetic Compatibility, volume 20, No 2, pp.296-305, May 1978.

[37] Ward Wallyn, frank Olyslager, Eric Laermans, Daniel De Zutter, "Fast evaluation of the shielding efficiency of rectangular shielding enclosures," International Symposium on Electromagnetic Compatibility Record, pp.311-316, august 1999.

[38] J. L. Norman Violette, Donald R. J. White, Michael F. Violette, "Electromagnetic Compatibility Handbook," 1991.

[39] Jacques Rollin, EMC Discipline Leader, CMAC Engineering, Kanata, Ontario, Canada.

APPENDIX A

Table A-1: EMC design Process

Product Definition	Preliminary EMC analysis	Physical review	Pre-Compliance verification	Compliance verification
Review product concept Define global standard requirements Perform an architecture analysis and risk assessment Identify specific EMC	EMC guidelines Design specifications	Mechanical design files review. Technology, frequency, rise time, components information available	Prototype PCBs, subsystem or system pre-testing	EMC compliance test
Product concept defined Electrical and mechanical design concepts Intended customers	General design specification	Mechanical design review De-risk with prototypes and mock-ups	EMC assessment of prototype using various methods: E-H field probe, radiated measurements, conducted measurements	EMC test plan Fully equipped and operational system

APPENDIX B

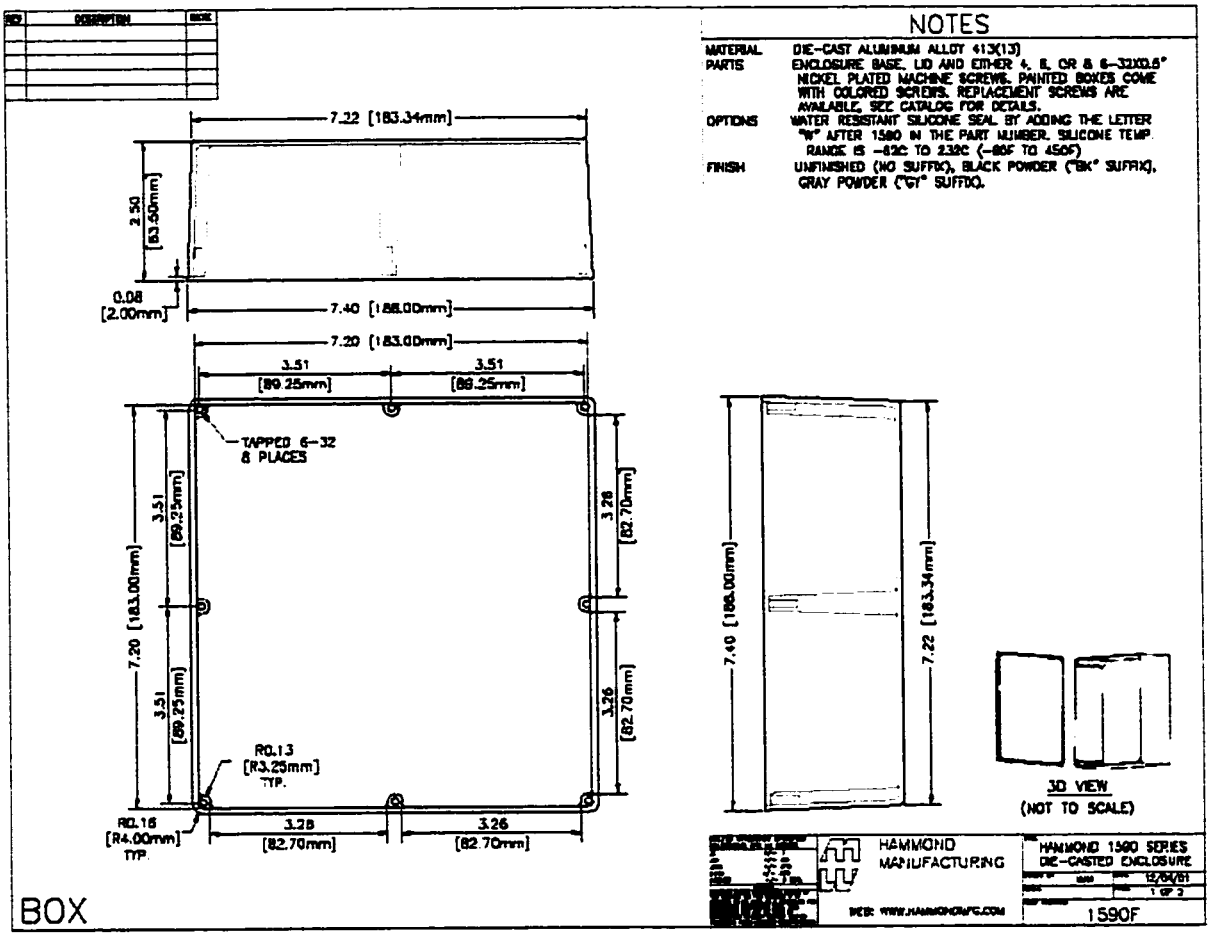

Figure B-1: Enclosure mechanical dimensions

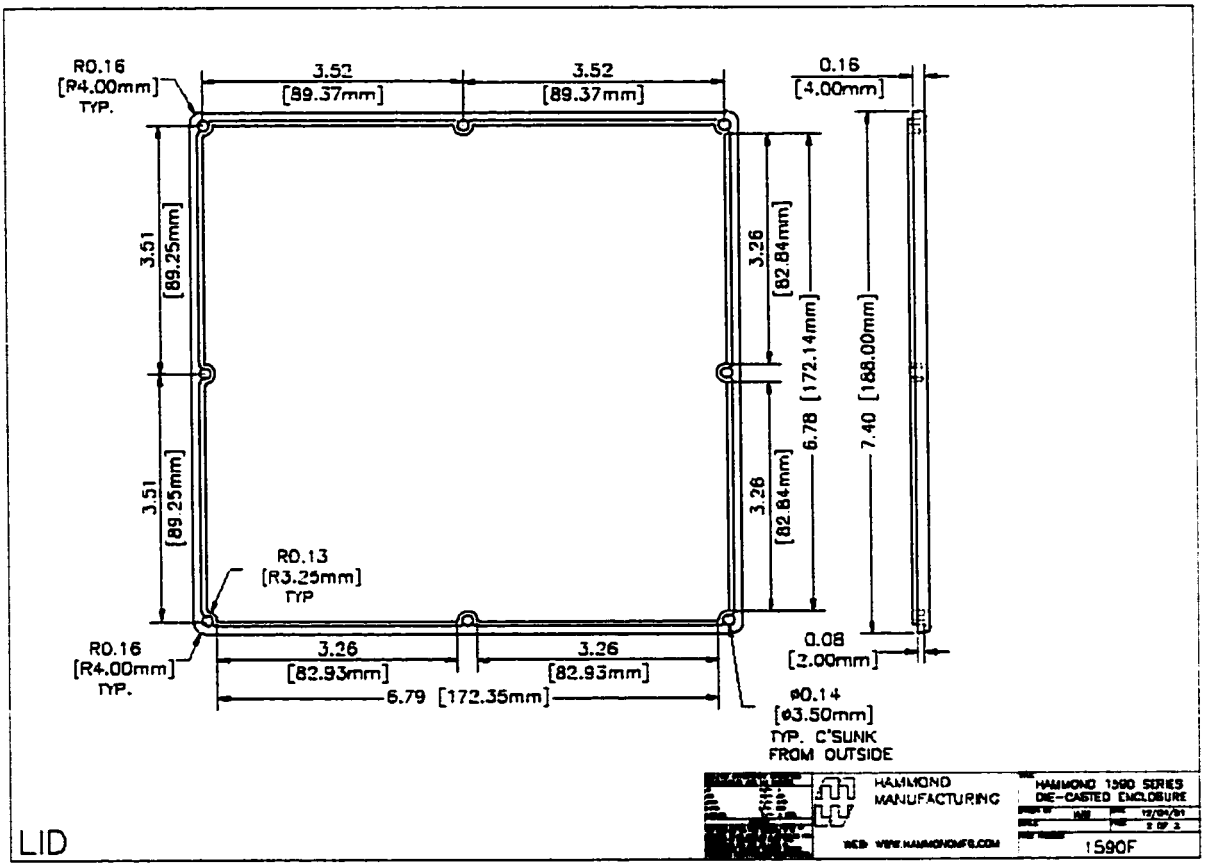

Figure B-2: Enclosure cover mechanical dimensions

APPENDIX C

C-1 Rectangular Aperture SE Estimate [19]

$$SE = \frac{1.2\times10^{12}\sqrt{\frac{V}{Q}}\ln(1+0.66\alpha)}{NL^3 f^{\frac{3}{2}}}$$

Where L is the slot length, α is the ratio of the slot length to the width of the slot, V is the volume of the enclosure, Q the quality factor and N the number of slots.

C-2 Honeycomb SE Estimate [38]

Operating wavelength in inches;

$$\lambda = \frac{30000}{f_{MHz}\,2.54} \qquad \text{(C-1)}$$

Attenuation in a single circular wave-guide below cut-off (dB);

$$K = \frac{6920}{d} \qquad \text{(C-2)}$$

Where d is the largest transverse dimension of the wave-guide in inches.

Attenuation in a single circular wave-guide below cut-off (dB);

$$P = 0.0046 L f_{MHz} \sqrt{\left(\frac{K}{f_{MHz}}\right)^2 - 1} \qquad \text{(C-3)}$$

where L is the depth of the wave-guide.

SE for a circular wave-guide honeycomb panel (dB);

$$20\log\left(\frac{\lambda}{2d}\right) - 10\log(N) + P \qquad \text{(C-4)}$$

Where N is the numbers of hole in the panel.

Equation (C-4) is base on a circular wave-guide, however it is applicable to Hexcell honeycombs.

APPENDIX D

C-MAC Engineering EMC test facilities are accredited by the Standards Council of Canada (SCC) in accordance with the scope of accreditation outlined in SCC letter dated 2001-02-16. The Federal Communications Commission (FCC) in the United States also recognizes these facilities to be compliant with the requirements of Section 2.948 of the FCC Rules, as outlined in a letter dated June 25,1999.

Standards Council of Canada (SCC) 

APPENDIX E

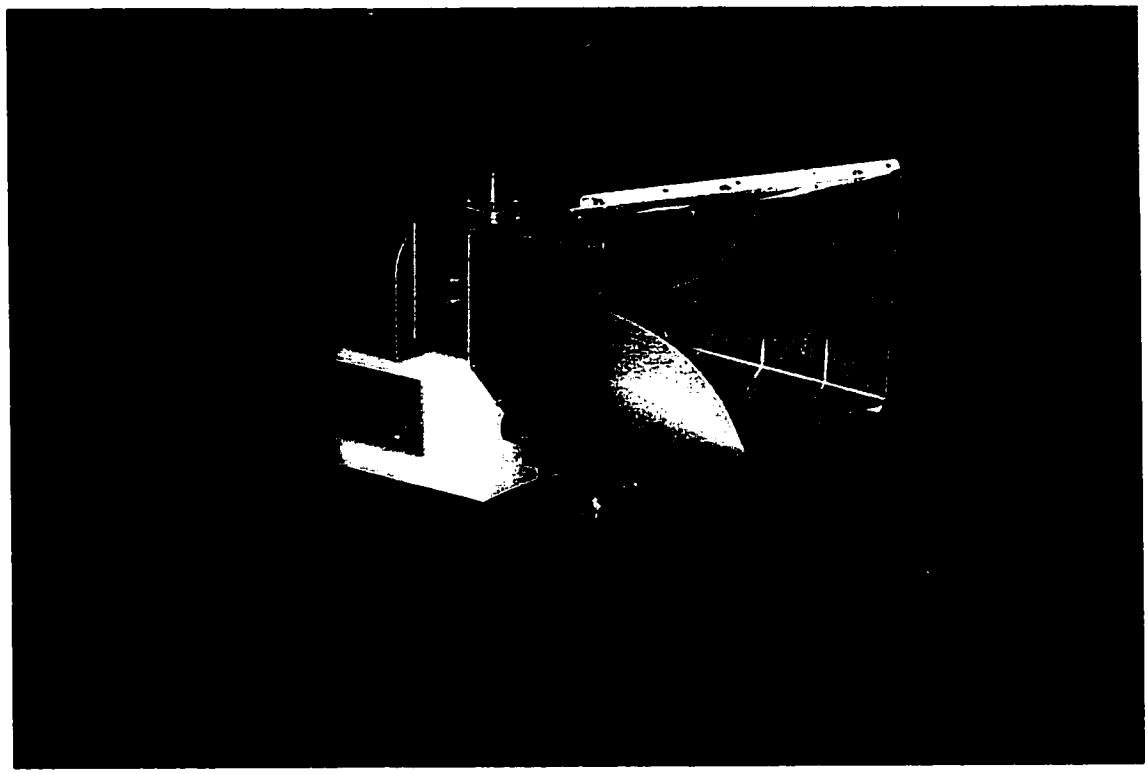

Figure E-1: Horn antenna

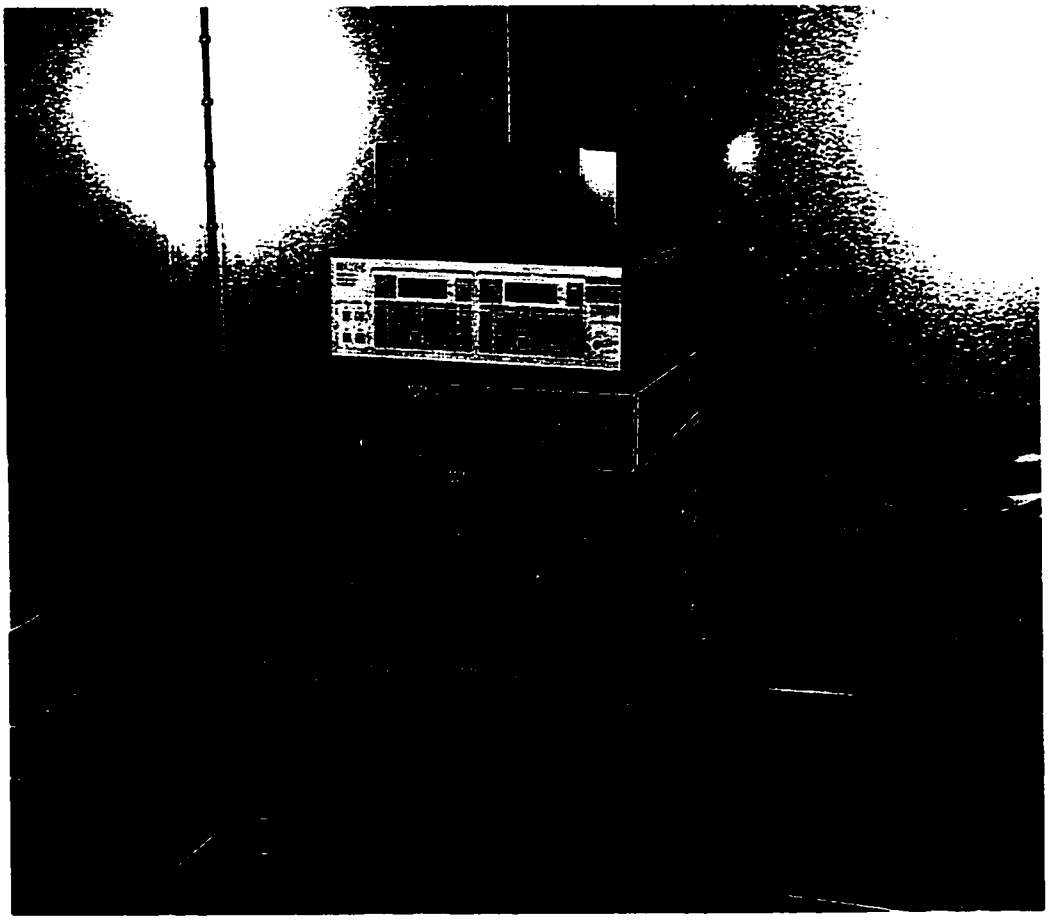

Figure E-2: Spectrum analyzer

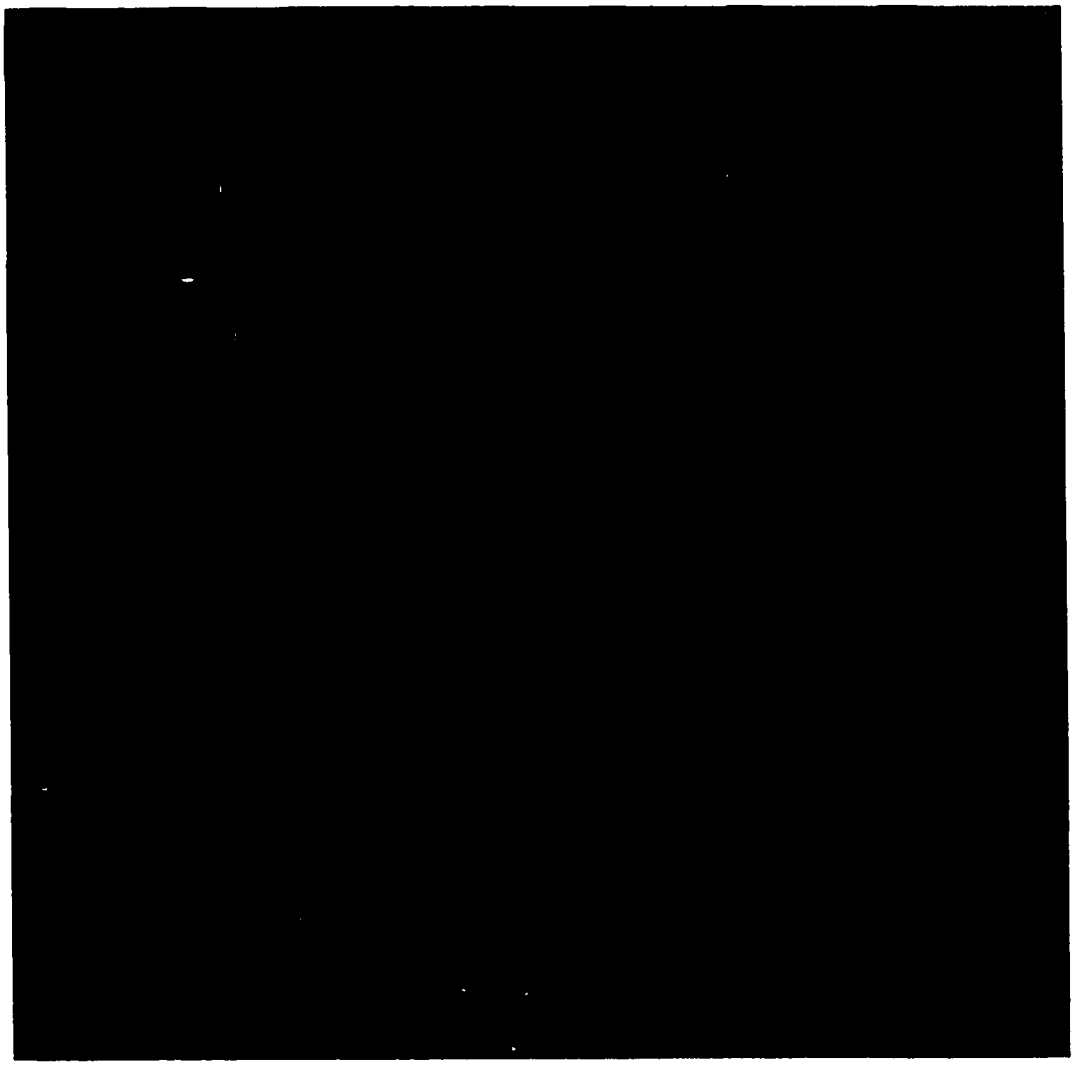

Figure E-3: Setup front view

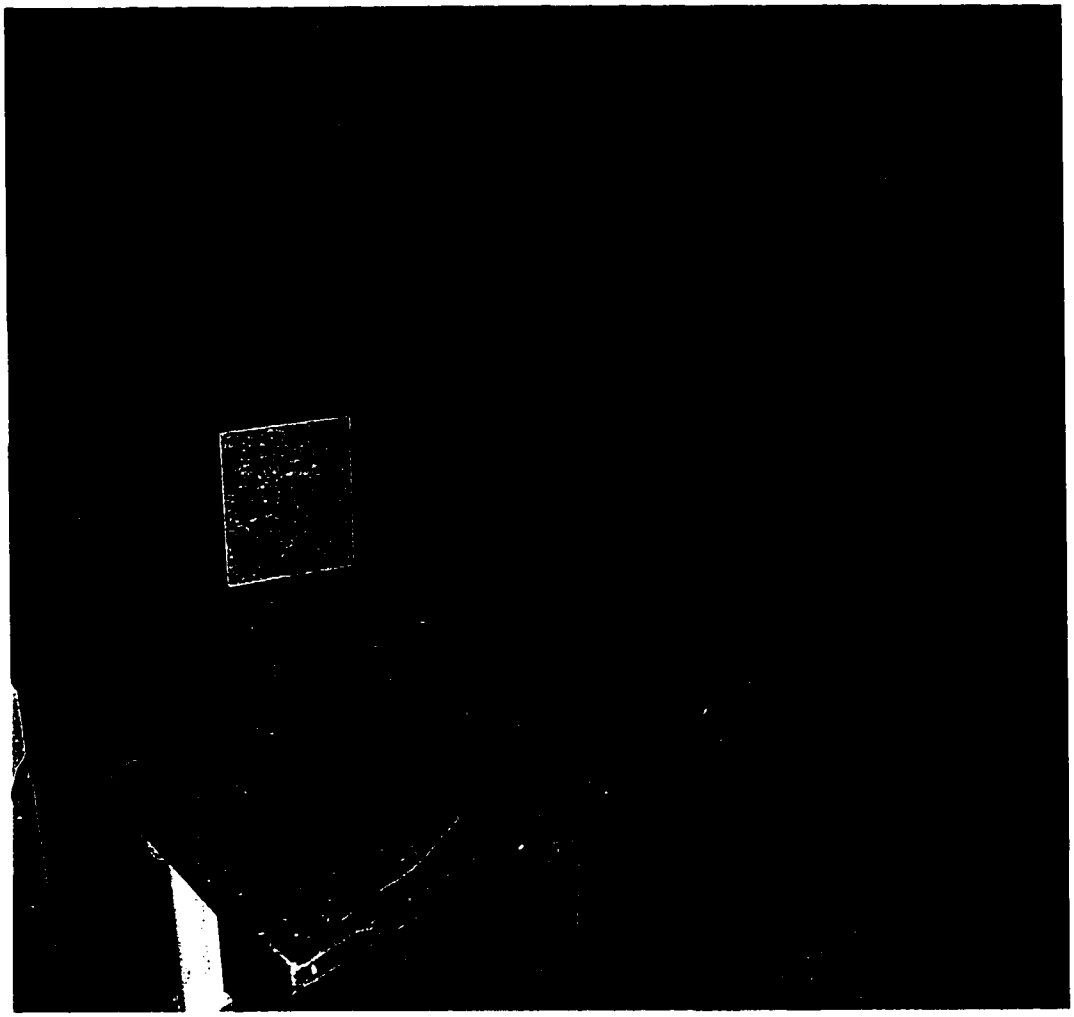

Figure E-4: Setup back view

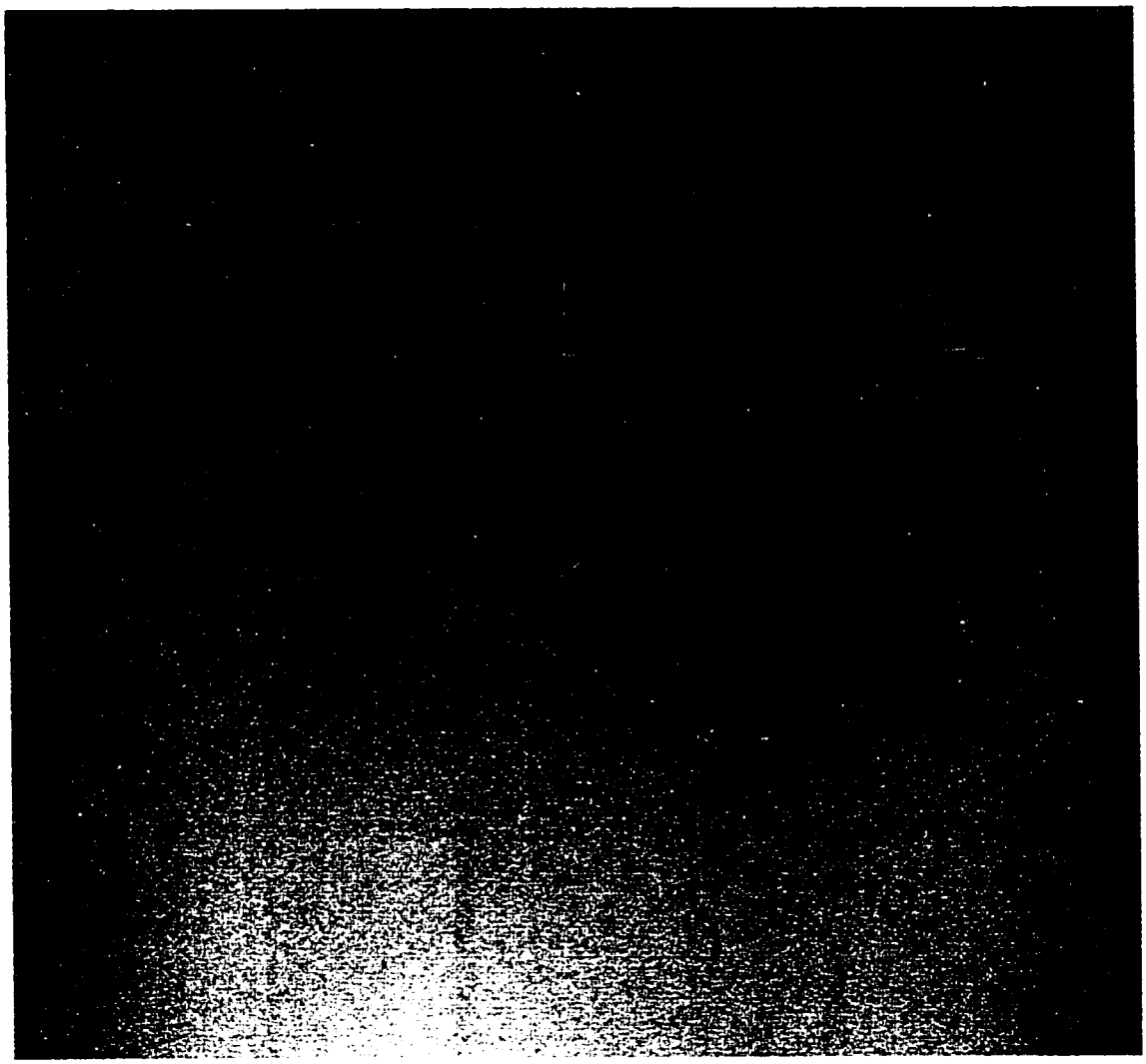

Figure E-5: Enclosure assembly

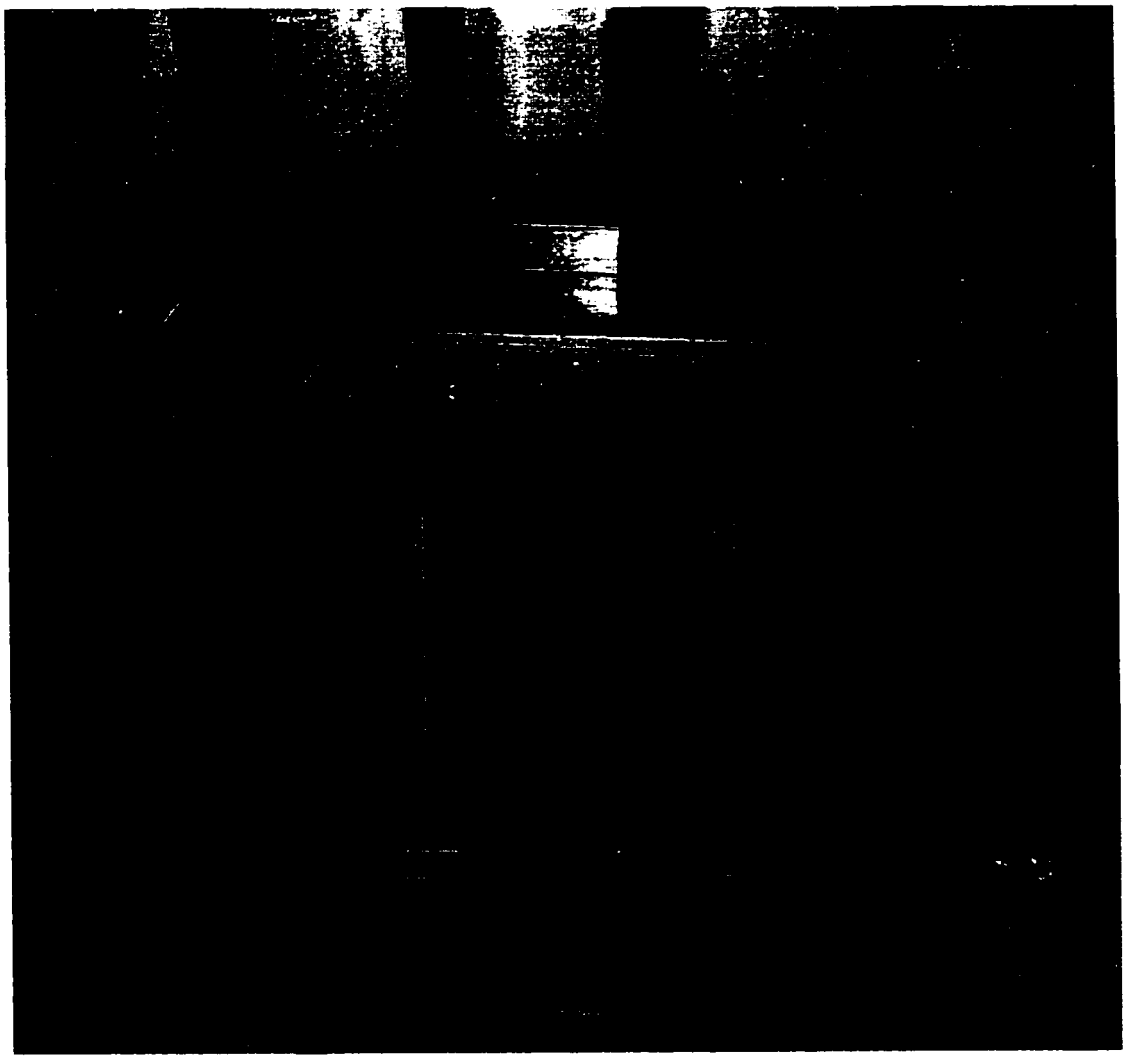

Figure E-6: Table setup

APPENDIX F

The battery noise source is built following [5] and using available parts. A voltage regulator L1529 is used to regulated the 7.1V coming from a video-camera battery. The second major part of the circuit is an amplifier, ERA 3SM DC-8GHz. A maximum of 12 dBm output can be achieved. The last and most important part of the circuitry is the ECL (clock). A 622.08 MHz clock is used in our circuit and can be changed if other ECL frequencies are available. The square shape coming out of the ECL is the perfect candidate to generate harmonics of 622.08 MHz. The antenna chosen for our experiment is a loop antenna. The loop antenna was designed for a portable phone. Schematic of the antenna and the noise source circuitry is presented in figures below.

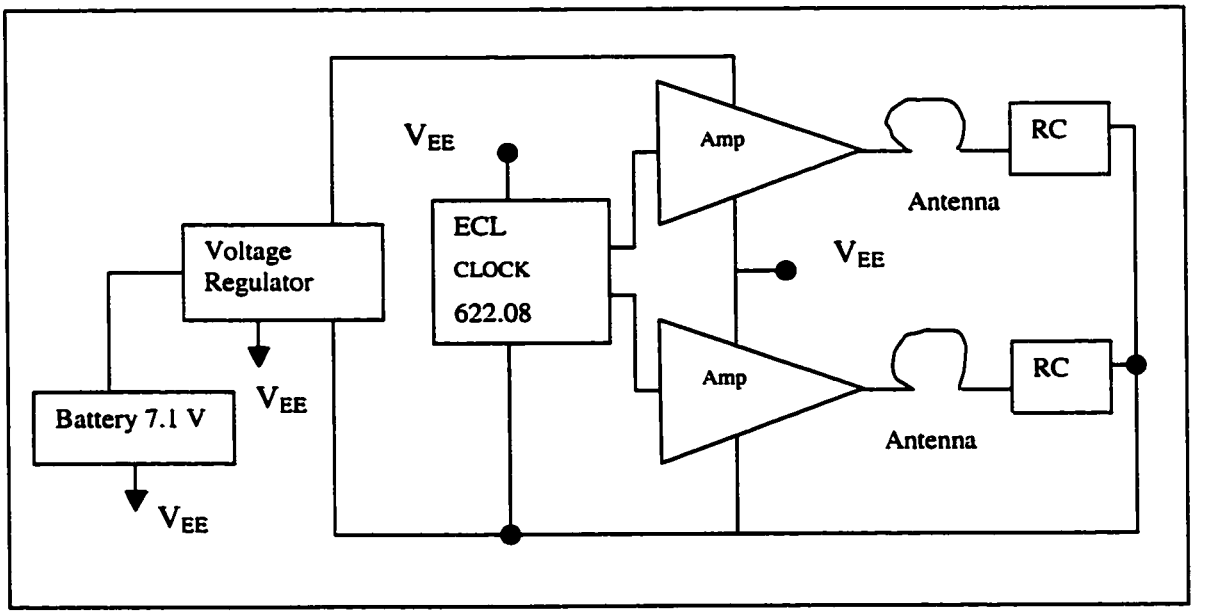

Figure F-1: Noise source circuitry.

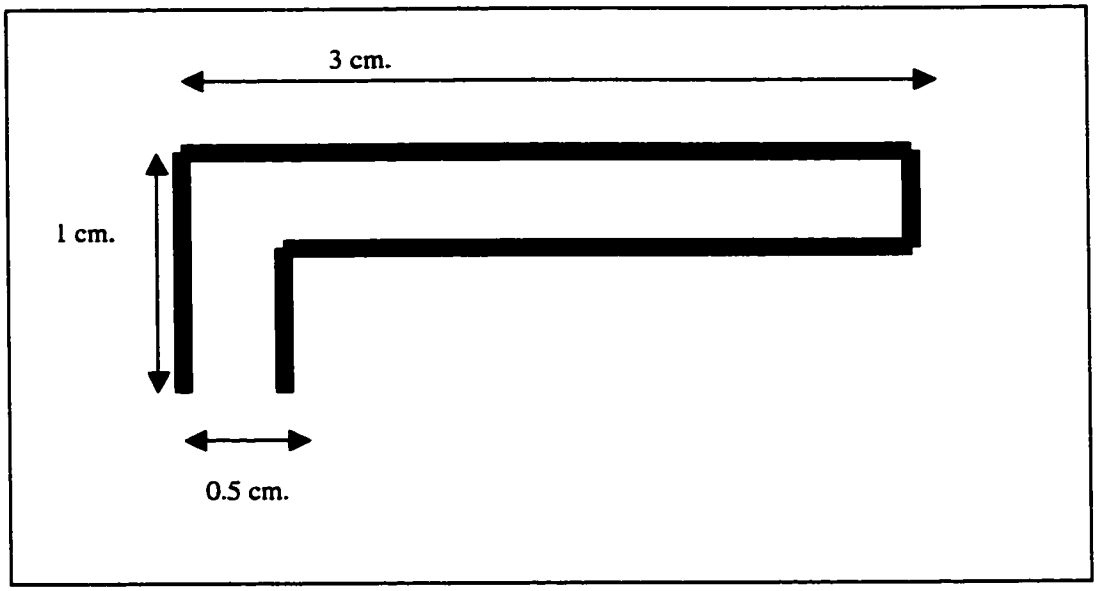

Figure F-2: Antenna dimensions

APPENDIX G

FDTD model MAK file of test case study without PCB

```
CM Rectangular Box with a Hole in the Cover No PCB
CE
FR 622.08
CM
EPSILONR    1   00.000  1 PEC
SIGMA       1   00.000
ME
CM
PLANEWAVE 90. 90.  0. 1.  0. 0.
CM
CM
CM
HLOBOX 0  1  -6.35  -9.4   -9.4  6.35   18.8  18.8   0.4
CM
XCYL 0  0. 0. -0.4 0. 1.27
CM
GE
CM
CM Cell size in CM
CELL  0.2
CM
WHITESPACE  10
TIMESTEPS  2048
MAKENE  EX   YZ   -2.775
CM YZ plane through the center of the box
MAKENE  EZ   XZ   0.
MAKENE  EZ   XY   0.
MAKENE  EZ   YZ   0.
CM
EN
```

FDTD model MAK file of test case study with PCB

```
CM Rectangular Box with a Hole in the Cover
CE
FR  622.08
CM
EPSILONR     1   00.000  1 PEC
SIGMA        1   00.000
ME
CM
PLANEWAVE 90. 90.  0. 1.  0. 0.
CM
CM
CM
HLOBOX 0  1  -6.35  -9.4   -9.4  6.35   18.8  18.8   0.4
BOX  1  -3.55  -8  -8  0.2  16  16
CM
XCYL 0  0. 0. -0.4 0. 0.635
CM
GE
CM
CM Cell size in CM
CELL  0.2
CM
WHITESPACE  10
CM
TIMESTEPS   2048
MAKENE EX   YZ   -2.775
CM YZ plane through the center of the box
MAKENE EZ   XZ   0.
MAKENE EZ   XY   0.
MAKENE EZ   YZ   0.
EN
```

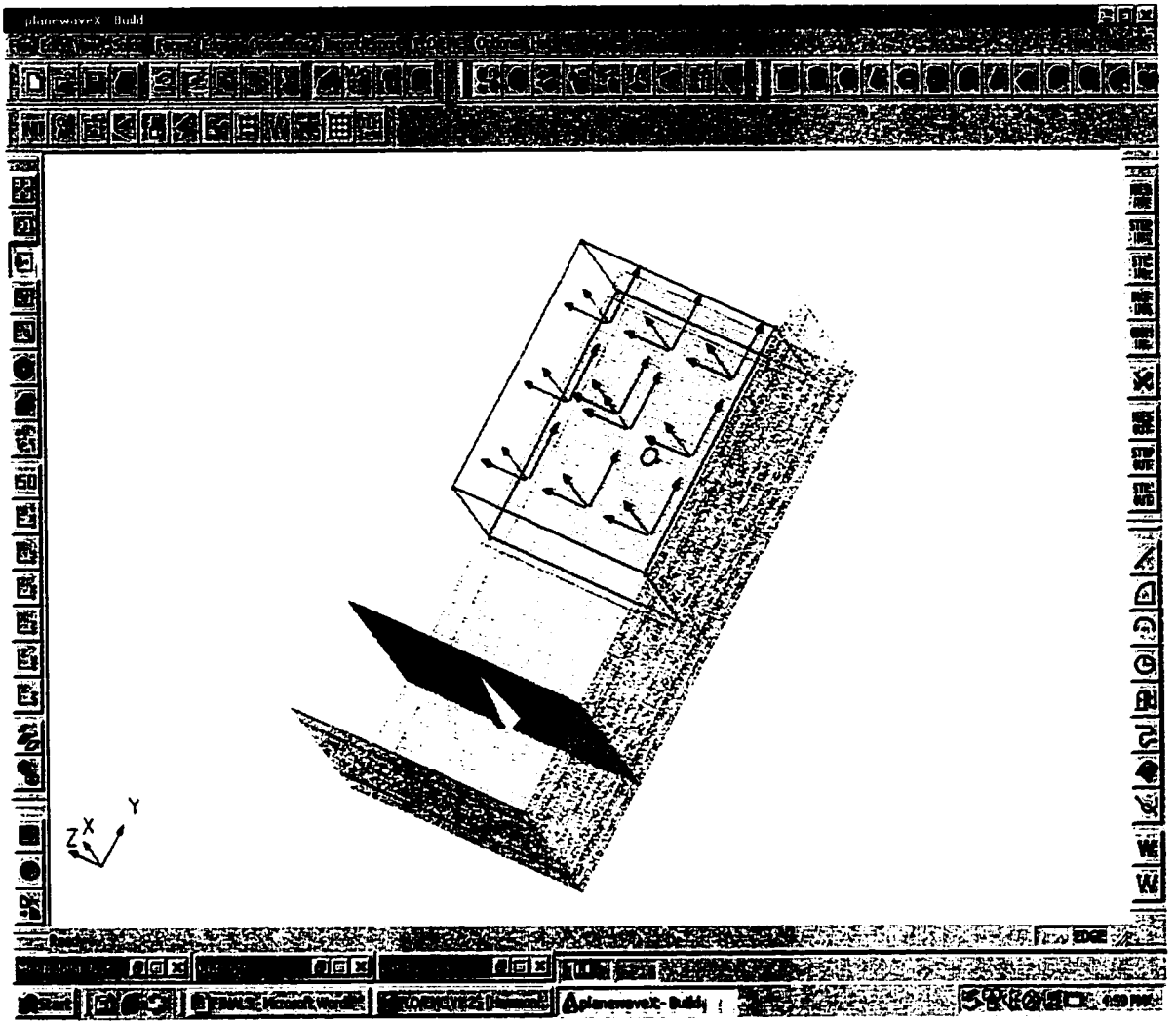

Figure G-1: TLM model of the enclosure without PCB

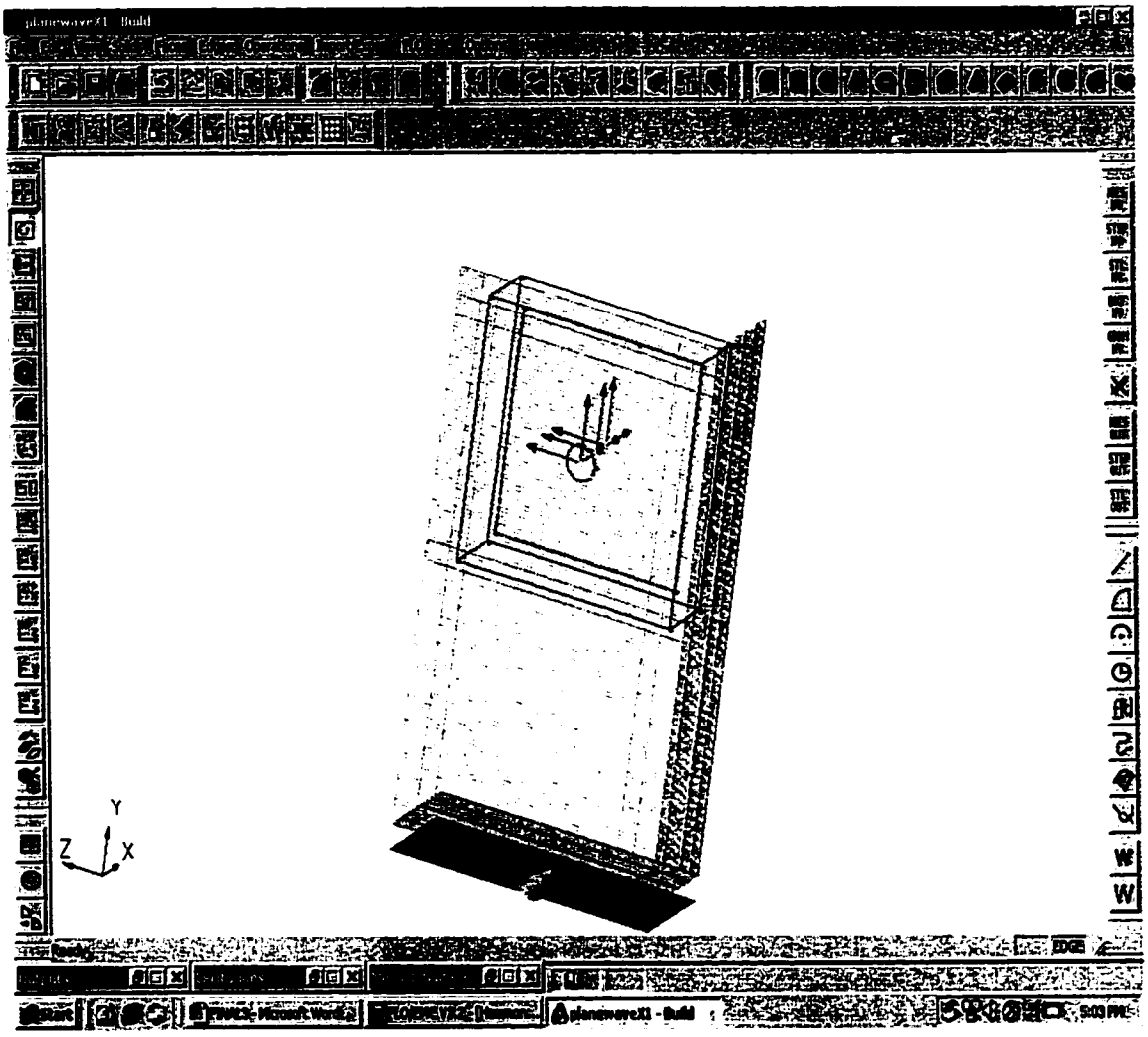

Figure G-2: TLM model of the enclosure with PCB